Alma Mater Studiorum - Università di Bologna

DIPARTIMENTO DI ASTRONOMIA
Corso di Dottorato di Ricerca in Astronomia
Ciclo XX (2005-2007)

A spectroscopic and photometric study of MSP companions in Galactic Globular Clusters

Dottorando:
Dott. Gabriele Cocozza

Relatore:
Ch.mo Prof. Francesco R. Ferraro

Coordinatore:
Ch.mo Prof. Lauro Moscardini

Scuola di Dottorato in Scienze Matematiche, Fisiche e Astronomiche
Settore Scientifico Disciplinare: Area 02 - Scienze Fisiche
FIS/05 Astronomia e Astrofisica

Contents

Chapter 1

Introduction

This Thesis is devoted to the study of the optical companions of Millisecond Pulsars in Galactic Globular Clusters (GCs) as a part of a large project specifically dedicated to the study of the environmental effects on passive stellar evolution in galactic GCs.

GCs are spherical systems of $10^5 \div 10^6$ Population II stars bound by their self-gravitation. Following a simple theoretical approach (Renzini & Buzzoni, 1986), all stars into a GC are formed at the same time during the collapse of a single molecular cloud, and, at a first approximation, they show the same chemical composition: this means that, excluding some effects as the stellar rotation, the magnetic field, or stars bound in binary systems, the differences in stellar evolutionary stages are only due to differences in the initial mass. The most massive stars evolves in few $10^6\ yr$ out of the main sequence, and eventually explode as type II supernovae, while less massive ones will lie in these systems for more than $10 \div 15\ Gyr$.

A similar stellar aggregate is the best approximation of the so-called Simple Stellar Population (SSP). At present, about 150 globular clusters are known in the Milky Way (Harris, 1996) [1], with ages of about 10-13Gyr (see for example the review by Carretta et al., 2000).

Nevertheless, recent advances in theory and observations have suggested that the

[1] When referencing to Harris (1996) we used the updated dataset at `http://www.physics.mcmaster.ca/Globular.html`

evolution of the stellar content in a GC is not simply passive: physical interactions between single stars as well as the formation, evolution, survival, and interactions of binary systems, have a significant influence on cluster stellar populations (Chernoff & Weinberg, 1990). Binaries can be created and destroyed, affecting the characteristics of the binary stellar population (Heggie, 1975) leading to the formation of "peculiar" objects, whose origin can not be explained via "*normal*" stellar evolution.

In fact advances in observational techniques have revealed the presence of a multitude of peculiar objects in GCs, including Millisecond Pulsars (MSPs), Blue Straggler Stars (BSS), bright and dim X-ray sources as Low Mass X-ray Binaries (LMXB) and Cataclysmic Variables (CV). The formation of these objects can not be explained in terms of the evolution of isolated stars, but they are thought to be the result of dynamical interactions, which take place in the densest regions (up to 10^6 stars per cubic parsec) of the clusters.

Direct physical collisions can produce Blue Straggler Stars (Lombardi Rasio & Shapiro, 1996), but near encounters are even more common and are thought to produce the majority of exotic objects into GCs. In this latter case the operating mechanism is believed to be the 2-body "tidal capture" (Fabian Pringle & Rees, 1975). This term indicates the outcome of a close encounter between a degenerate object (neutron star or white dwarf) and a main sequence star or a red giant. During such an encounter, strong tides are raised on the surface of the non-degenerate star. These distortions dissipate orbital energy and can therefore result in capture of the non-degenerate star and the formation of a close-binary. Tidal capture nicely accounts for the observed overabundance of low mass X-ray binaries (LMXBs) and MSPs in GCs, relative to the galactic field.

The continuous formation and destruction of binaries can affect the dynamics of the cluster as a whole. As a result it is now clear that stellar evolution and stellar dynamics can no longer be studied separately.

Binary systems play a fundamental role also on the overall evolution of a cluster: because of the gravitational interactions among stars, GCs dynamically evolve on time scales generally smaller than their ages. The first signature of a dynamical process within a GC is mass segregation: more massive stars (as neutron stars, binaries, binary by-

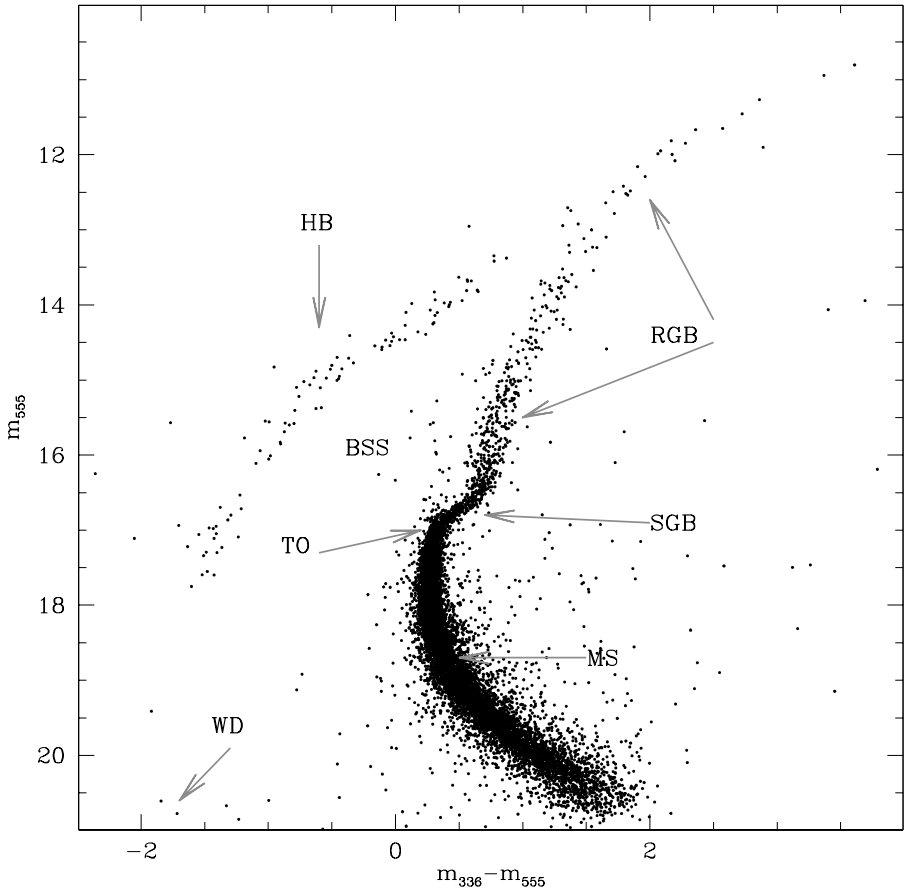

Figure 1.1: $F555W, (F336W - F555W)$ Color-Magnitude Diagram of the Galactic Globular cluster NGC 6752. Normal evolutive sequences are indicated together with the position of some peculiar objects such as Blue Straggler Stars. Note that some stars lies between the main sequence and the cooling sequence of white dwarfs. These objects can be binary systems with a blue excess, as Cataclysmic Variables.

products) should settle toward the center.

Moreover, even more dramatic dynamical events can occur during the cluster's lifetime; in fact due both to the distribution of energy between single stars within a GC and to the interaction with nearest stars, some stars can obtain velocities larger than the escape velocity, and cross the tidal boundary removing energy from the cluster. This fact induce a substantial change in the structure of the cluster itself, leading the inner region to shrink and increasing the average velocity of the stars. This runaway process is called *gravothermal collapse* (Lynden-bell & Wood, 1968) and would lead to the collapse of the core: about 15% of GC shows evidence for this phenomenon.

To reverse the collapse of the core, energy must be added to the GC; mass loss acts as energy source reducing the total binding energy per unit of mass and therefore increasing the velocity dispersion with respect of the virial equilibrium value. The three most important causes of mass loss are stellar evolution, especially for the most massive stars in the early life of the cluster, merging of stars, and escape from the cluster of weakly bounded stars (Goodman, 1989). However binary systems are the most important energy source; binaries in the core of the cluster countinuosly interact with single stars, converting binding energy of the binary system into kinetic energy of the single star, and reverse the collapse of the core. In fact, during a collision, part of the orbital energy of a binary system is transferred to the passing single stars, while the binary system itself will become highly hardened (i.e., tightly bound). This close binaries are the heat sources that causes expansion and evaporation, while binary-binary collisions can halt (or, more probably, delay) the collapse of the core avoiding infinite central density: during this phase most of the binaries in the core will be "burned" (= destroyed) by close encounters (Hut et al., 1992).

The onset of energy generation in the core of a GC marks the end of the collapse phase, and the core can undergo a re-expansion; this expansion can lower both the central temperature (= kinetic energy), and the density of the core. The expanding region in the cluster center will grow radially until it reaches a region of radially decreasing temperature. At this point the expansion halt, and the central region starts to collapse again (Bettwieser & Sugimoto, 1984). These authors suggested that many GCs may already

have undergone an initial core collapse and are presently oscillating gravothermally. The non linear nature of these oscillations would imply that the cores spend most of their time near the maximally expanded stages, during which the clusters may have normal appearance with finite-size core. In GC evolution it is the formation of binaries, and their subsequent "burning" during encounters with single stars, which releases the energy which can counteract the gravitational contraction (Hut et al., 1992). Then, when a GC (particularly if it has a large primordial binary population) begins the core-collapse phase, the production of collisional by-products in the cluster "furnace" should reach its maximum.

The presence of binaries in GC was clearly proved by the first observation of the X-ray satellites *Uhuru* and *OSO-7* (Giacconi et al., 1974; Clark, 1975). These pioneering works showed that the bright X-ray sources (with $L_X > 10^{36} ergs^{-1}$) discovered in Globular Clusters, represented a significant overabundance when compared to the sources in the Galactic field. Altougth these globular clusters contain $\lesssim 0.1\%$ of the stellar contents with respect to our Galaxy, they contain $\gtrsim 10\%$ of the bright X-ray sources (Katz, 1975).

It was soon realized that these sources were Neutron Stars (NS) accreting matter from a stellar companion in a binary system (the systems today called Low Mass X-ray Binaries), and that these sources were likely to be formed trough dynamical interaction (Clark, 1975), either trough three body interaction or tidal capture (Fabian Pringle & Rees, 1975).

Altought a large number of bright X-ray sources was discovered starting more than 30 years ago, not many binary systems were known at the time. This was essentially due to selection effects: spectroscopic radial velocity studies could only monitor a few bright giants stars, and photometric observations suffered from crowding in the dense globular clusters core. As a consequence, just few dozen binaries were clearly identified before the early '90.

Influence of dynamical evolution on stellar populations

For all the reasons illustrated above, GC studies have found many applications in astrophysics:

1) They are ideal laboratories to carry out "controlled experiments" in stellar structure and evolution.

2) Being very bright, they can be detected also at very large distances, and used as tracers of the structure and evolution of a galaxy as a whole: Shapley (1918), for instance, used the distribution of these stellar systems to determine the shape of our Galaxy.

3) Due to their large stellar content ($10^5 \div 10^6$ stars) the dynamics of the stars within a GC is an excellent application for the classical gravitational n-body problem.

Furthermore GCs provide an ideal laboratory to study stellar dynamics. Interactions between individual stars establish a sort of equilibrium on a time scale that is typically $\lesssim 10^{10}\,\mathrm{yr}$ at the half-mass radius, and $\lesssim 10^{8}\,\mathrm{yr}$ in the core. The intrinsic instability of self-gravitating systems precludes any final equilibrium state in a GC.

In the '80s, CCD observations allowed a systematic investigation of the inner surface brightness profiles (within $\sim 3'$) of 127 galactic GCs (Djorgovski & King, 1986; Chernoff & Djorgowski, 1989; Trager King & Djorgovski, 1995). Djorgovski & King (1986) sorted GCs into two different classes:

- the "King model clusters", whose surface brightness profiles near the center resemble a single component King model (King, 1966) with a flat isothermal core and a steep envelope

- the "collapsed-core clusters", whose surface brightness profiles follow an almost pure power law with an exponent of about -1. About the 20% of the galactic GCs exhibit apparent departures from King-model profiles, consequently they are considered to have a collapsed core.

The current equilibrium stage of a GC is well described by the King model (King, 1966), which best fit the surface brightness and/or density profile. The King model is a Maxwellian distribution function, with a cut-off in phase space of stars velocity: the

tail of stars with energy larger than the escape energy from the system is truncated. As a result of the cut-off in the distribution function, the models are finite in mass and size. King's models depend on three dimensional parameters: the central density ρ_c, the central velocity dispersion σ_c and the tidal radius r_t. A usefull dimensionless parameter is the so-called *concentration* parameter, defined as

$$c = \frac{r_t}{r_c} \quad being \quad r_c = \frac{3\sigma}{\sqrt{8\pi G\rho_0}}. \tag{1.1}$$

In an attempt to identify correlations among structural and dynamical parameter of GCs, Djorgovski & Meylan (1994) noted that the most concentrated clusters have ratios r_c/r_h (where r_h is the half-light radius, i.e. the radius that contains half of the cluster light and consequently $\sim$ half of the cluster mass) of a few percent.

Clusters with higher concentrations and smaller and denser cores are presumably more dynamical evolved. By considering a database of 143 galactic GCs Djorgovski & Meylan (1994) revealed a correlation between the luminosity and the concentration of the GCs. These authors noted that there is no obvious reason why dynamical evolution would produce a correlation between luminosity and concentration, unless to consider differential survival effects: less massive clusters would evaporate faster in the tidal field of the Galaxy, while more massive clusters would on average survive longer, and have better chances of reaching a more evolved status.

A relation between the volume luminosity densities (ρ_0) and r_c was noted (Lightman, 1982; Djorgovski & Meylan, 1994). While a core shrinks, the GC mass changes a little, or decreases slightly due to an enhanced evaporation of stars. Simple models of gravothermal catastrophe (core-collapse) for isolated cluster predicts a scaling law $\rho_0 \sim r_c^{-2.23}$ (Lynden-Bell & Eggleton, 1980; Cohn H., 1980), close to the observed scaling $\rho_0 \sim r_c^{-2.60\pm0.15}$, within the observed errors (Djorgovski & Meylan, 1994). The observed relation is, however, steeper, possibly due to tidal effects: less concentrated clusters with larger cores would be more susceptible to evaporation of stars, which would lower their densities.

In the Galactic system, the smallest GCs cores have $\rho_c \sim 0.05\,\mathrm{pc}$, and $t_{rc} \sim$

$10\,t_{cross} \sim 10^5\,\mathrm{yr}$ (Djorgovski & Meylan, 1994). They must be dynamically highly evolved, and can hardly be much smaller, since $t_{rc} \geq t_{cross}$ must hold. The distribution of relaxation times agrees with theoretical expectations, and it allows to derive the rate of core collapse and GC evaporation within the Galaxy (Hut & Djorgovski, 1992)

King models provide accurate fits to the cores for the majority of GCs, but for all those GCs, which are undergoing, or have undergone, the core collapse, an excess in the observed counts, with respect of the king model is clearly observable.

It is now commonly accepted that the presence of also a few percent of binaries in the core of a GC can influence the dynamical evolution of the cluster as a whole: in particular they can affect the later phases of core collapse in a GC and may lead to a core expansion. Binary stars can form in a cluster in three distinct ways:

- binaries may be primordial;
- they may be formed during a three-body encounter if the third star carries away sufficient kinetic energy to leave the other two bound;
- they may be formed in two-body encounters if the stellar encounter occurs within a few stellar radii and tidal dissipation results in capture.

The latter two species of binaries are expected to be relatively more abundant in the core of GCs, with respect of the outskirts, both because the conditions are more favorable for forming them in the higher density regions, and because they are on average more massive than single stars and therefore tend to sink toward the cluster center. If it is evident that stellar interactions can strongly influence the dynamical evolution of a GC; suspicious that stellar dynamics may influence the stellar evolution in GCs have more than three decades old (Renzini, 1983), and it is now commonly know that GCs stellar populations exhibit numerous observable "*peculiar*" objects which testify the influence of stellar dynamics on stellar populations.

These effects can both alter the normal evolutive sequences (i.e. they can lead to the formation of long blue horizontal branch tails, or alterate the red giant branch luminosity function), and generate new "peculiar" objects (as Blue Straggler stars, low-mass X-ray

binaries, millisecond pulsars, etc.), whose origin can not be described as the evolution of a normal star.

In this framework the Department of Astronomy of the Bologna University, in collaboration with other institutions (Astronomical Observatory of Cagliari and Bologna, University of Virginia) have started a long-term program aimed to study the possible link between the dynamical evolution of GCs and the evolution of their stellar populations.

In this thesis, in particular, we have focused our attention on the companion to binary MSPs, in order to fully understand the formation mechanisms and the evolution of such systems in GCs.

The Thesis is organized as follows:

Chapter 2 presents a description of the characteristic of MSPs in Galactic GCs.

Chapter 3 is devoted to the analysis of the spectroscopic and photometric properties of the companion to the millisecond pulsar PSR J1911-5958 in the Globular Clusters NGC 6752.

In Chapter 4 we report the discovery of the peculiar companion to the eclipsing Millisecond Pulsar PSR J1701-3006B in the globular cluster NGC6266.

Some of the results presented in this Thesis have been already published in refered journals and conference proceedings. We list them in the following.

- **Cocozza, G.**, Ferraro, F. R., Possenti, A., & D'Amico, N. " The puzzling properties of the Helium White Dwarf orbiting the millisecond pulsar PSR J1911-5958 in NGC 6752" 2006, ApjL, 641, L129

- **Cocozza, G.**, Ferraro, F. R., Possenti, A., D'Amico, N. "The properties of the He-WD orbiting the Millisecond Pulsar J1911-5958 in NGC 6752" 2007 AIPC, 924, 641

- Possenti, A., Corongiu, A., Manchester, R., Camilo, F., Lyne, A., D'Amico, N., Sarkissian, J., Ferraro, F.R., & **Cocozza, G**, " The Timing of Globular Cluster Pulsars at Parkes" 2006, ChJAS 6, 176

- **Cocozza, G.**, Ferraro, F. R., Possenti, A., Beccari, G., Lanzoni, B., Ransom, S., Rood, R.& D'Amico, N. " Discovery of a tidally deformed millisecond pulsar companion in NGC 6266" 2008, ApJL submitted

Chapter 2

The Millisecond Pulsars Population

A neutron star (NS) is an ultracompact object (with a mean density $< \rho > \gtrsim 10^{14}\,\mathrm{g\,cm^{-3}}$) formed during the supernova explosion of a massive star, heavier than $M \gtrsim 8 - 10 M_{\odot}$.

After the explosion a NS is characterized by a very short spin period ($P_{in} \sim 10^{-2}\ sec$) and a very high magnetic field $B \sim 10^{13}\ gauss$.

The tremendous magnetic moments and the fast spinning rates allow the young NS to emit at radio frequencies. With a favorable geometry in which the magnetic moment is not aligned with the rotational axis, and the cone of the radio emission is direct toward the Earth, this kind of objects appear to us as radio millisecond pulsars. If Ω is the angular velocity of the neutron star and B_p the dipole magnetic field strenght, the neutron star emits electromagnetic waves $\dot{E}$ given by the simple "lighthouse" model (Pacini, 1967)

$$\dot{E} = -\frac{2 d_m^2 \Omega^4 sin^2\beta}{3c^3}, \quad with \quad d_m = \frac{B_p R^3}{2} \tag{2.1}$$

where d_m is the magnetic moment of the star expressed as a function of its radius R and the magnetic field strength B_p and β is the angle between the magnetic and the spin axes. The rotational energy of an homogeneusly rotating star is

$$E = \frac{I\Omega^2}{2} \tag{2.2}$$

and depend on the moment of inertia of the star I. If the electromagnetic waves are emitted at the expense of the rotational energy losses $\dot{E} = I\Omega\dot{\Omega}$, one can infer the magnetic field of the radio pulsar by measuring the spin period $P = 2\pi/\Omega$ and the spin down rate $\dot{P}$:

$$B_p^2 = -\frac{I\dot{\Omega}}{A\Omega^3} = \frac{IP\dot{P}}{4\pi^2 A}.$$

(2.3)

with the same measures is possible to estimate the characteristic age of the pulsar (also called spin-down age) that results:

$$\tau_c = \frac{P}{2\dot{P}} \tag{2.4}$$

Due to this radio–emission, pulsars lose energy and decelerate ($dP/dt > 0$), and after $\sim 10^7\,\mathrm{yr}$ the radio emission ceases. At this evolutionary stages also the magnetic field decays to $B \sim 10^{11} gauss$. In Fig.2.1 are shown all the inferred properties of the complete sample of radio pulsar today known, using the simple "lighthouse" emission model.

As a great number of stars, a large fraction of the NS progenitor belongs to a binary system: from the virial theorem, it follows that a binary system gets disrupted if more than half of the total pre-supernova mass of the system is ejected during the explosion (assuming a spherical symmetry). Moreover, the fraction of surviving binaries is affected by the magnitude and the direction of any impulsive "kick" velocity that the neutron star receives at birth (Hills, 1983; Bailes, 1989). Binaries disrupted from the explosion produce a high-velocity neutron star and an OB runaway star. The high probability of binary disruption during the explosion, explains why so few neutron stars in the galactic field (about 70 out to ~ 1700, less than 5%) have a companion: as shown in the §2.1, this percentage dramatically increase for the millisecond pulsars in globular clusters.

But if the old, silent neutron star is member of a binary system (either because the binary was not disrupted by the supernova explosion, or it acquires a companion during its following life) and if the companion star is massive enough ($M \gtrsim 1 M_\odot$), this companion evolve into a red giant and fill its Roche lobe. This starts a period of mass-transfer from the giant onto the neutron star, which is recycled to millisecond period (Alpar et al., 1982; Bhattacharya & van den Heuvel, 1991). During this period, which can last from a few

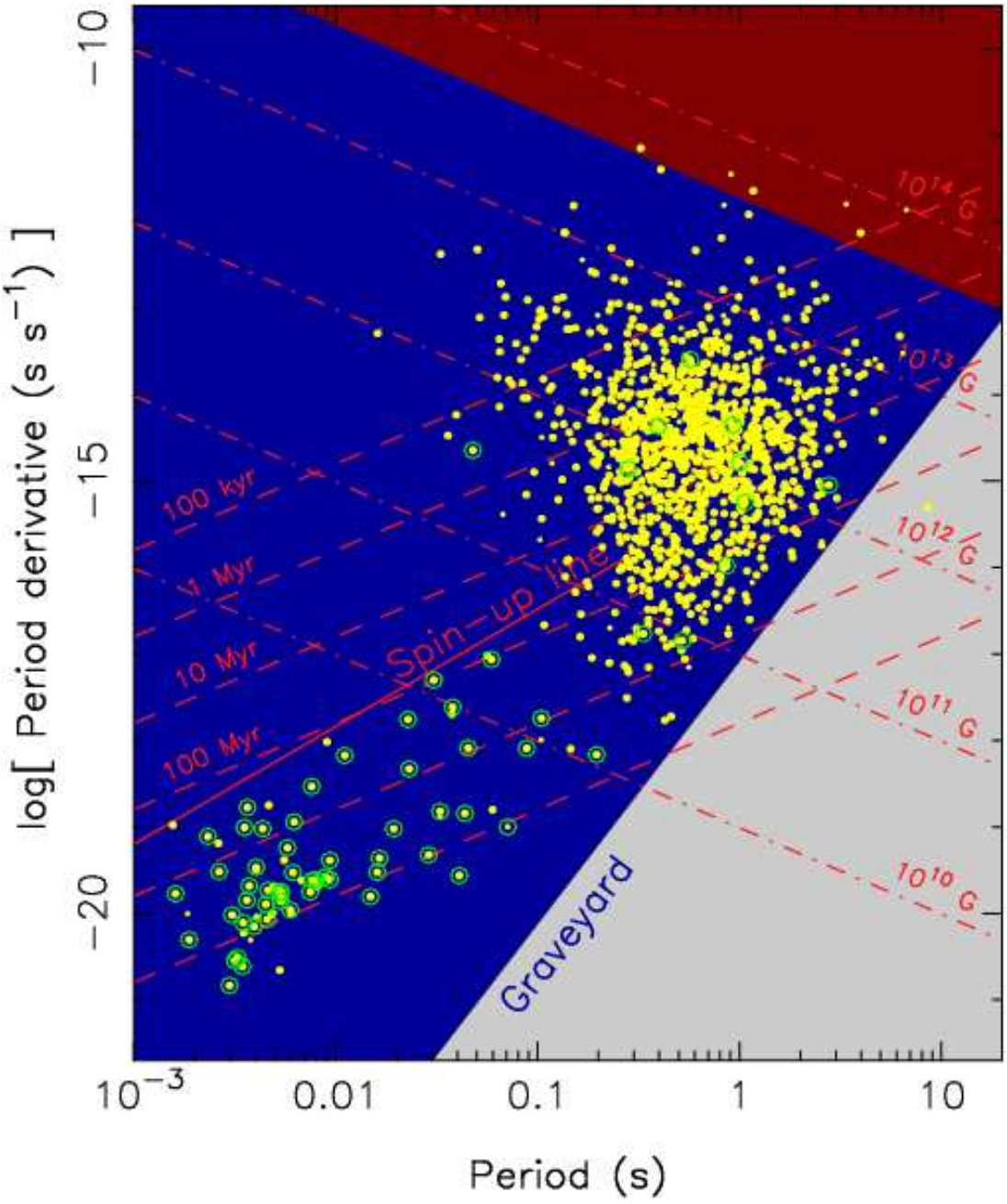

Figure 2.1: $P - \dot{P}$ Diagram showing the rotational parameters for the whole sample of radio pulsar in the galactic field, in galactic globular clusters and the Magellanic Clouds:pulsars in binary systems are highlighted by open green circles, red dashed line represent the spin-down age of the pulsar, whereas the red dash-dotted line shows the inferred magnetic field. The figure comes from the Lorimer 2005 review.

Myr to a few Gyr (Tauris & Savonije, 1999), depending on the companion mass, the mass falling onto the neutron star forms an accretion disk, emitting X-rays produced from the liberation of gravitational energy and this system can be observed as an X-ray binary.

The mass transfer process from the companion star also transfer very efficiently angular moment onto the neutron star surface, that is re-accelerated to very fast rotational period, tipically of the order of $10\,ms$. From the Fig2.1 we may understand the differences between the normal pulsars and the MSP population.

The $P - \dot{P}$ diagram tell us that the bulk of the pulsar population is characterized by spin period $P \sim 0.5 \div 1sec$, dipole magnetic field strenght $B \sim 10^{11 \div 12} gauss$, spin–down age $\tau_c \sim 10^7 yr$ and values of the spin period derivative $\dot{P} \sim 10^{-15} s\ s^{-1}$. Few object lies in the upper–left corner of the $P - \dot{P}$ diagram: they are the new–born pulsars, as the Crab or the Vela Pulsars, the youngest pulsars today known. This objects are also characterized by higher magnetic fields, faster spin periods and higher values of the spin period derivative.

A second group of pulsars lies in the lower–left corner in the Fig2.1: all these objects are characterized by faster spin period (tipically $1 \div 10ms$), lower magnetic field strenght and spin period derivatives ($B \sim 10^8 gauss$ and $\dot{P} \sim 10^{-19} s\ s^{-1}$ respectively) and larger spin–down age $\tau_c \sim 10^{9 \div 10} yr$. The large majority of these objects (highlighted with green open circles) have a companion, which plays a fundamental role to re-accelerate the pulsar up to a very short rotational periods. These objects are called MSP. The mass and angular momentum accretion onto the NS surface, is commonly called *recycling process*, and consequently the formation mechanism of a MSP starting with a binary systems hosting a NS and a normal star is the so-called *recycling scenario*(Alpar et al., 1982; Bhattacharya & van den Heuvel, 1991).

In high mass binary systems, in which the companion of the NS has a typical mass $M \gtrsim 8 - 10 M_\odot$, the normal star is massive enough to explode as a second supernova, producing a new neutron star. If the binary system survive also to the second explosion, the result is a rare double neutron star binary systems in a quite eccentric orbit. Less than ten of this systems are currently known, the first example being the *midly-recyled* PSR B1913+16 (Hulse & Taylor, 1974), a $59\ ms$ radio pulsar orbits its companion in $7.75\ hr$.

In the formation scenario briefly descrived above, PSR B1913+16 is an example of an old neutron star, having subsequently accreted matter and acquired angular momentum during the evolution of the companion out the main sequence.

For more than 30 years no one example was known in which also the second-born neutron star was observed as a radio pulsar. The discovery of the double pulsar PSR J0737-3039 system (Burgay et al., 2003; Lyne et al., 2004), harbouring a $22.7\ ms$ recycled pulsar (the pulsar "A") and normal $2.77\ s$ pulsar (the pulsar "B") orbiting every $2.4\ hr$, has now strongly confirmed the evolutionary model, in which the pulsar "A" and "B" are the first and the second born neutron stars respectively.

In low-mass X-ray binary sistems, the neutron star orbits with a companion having a lower mass ($M \lesssim 1 M_{\odot}$), which evolves on a much longer time-scale, spinning the neutron star up to periods shorter than $10\ ms$; tidal forces during this long phase serve to circularize the orbits. At the end of the accretion process when the mass envelpe of the companion star falls below a critical value ($\sim 0.05 M_{\odot}$, Driebe et al. 1999, Althaus et al. 2001), mass transfer stops and the core of the companion star will contract to a white dwarf, whereas the millisecond pulsar can be observed again in the radio band. The re-appearance of the radio emission marks the end of the accreting phase. This model has received strong support in the recent years after the discovery of the X-ray pulsations (with a periodicity of $2.49\ ms$) from the low mass X-ray burster SAX J$1808.4-3658$ (Wijnands & van der Klis, 1998). Six other "X-Ray Accreting millisecond pulsar" are now known, all with spin period shorter than $6\ ms$; despite intensive searches, no radio pulsation have been detected so far in these systems. Accreting millisecond pulsars could be the link between the bright low mass X-ray binary and the millisecond pulsar orbiting with an evolved companion. At the end of the recycling process we expect that MSP will orbits in a binary system with very light, almost exhausted star or, more commonly with a light Helium white dwarf, the core of a normal star that have lost the external envelope during the accretion phase. In the Fig.2.2 it's shows in a cartoon the formation mechanism for a millisecon pulsar starting with a different kind of binary systems.

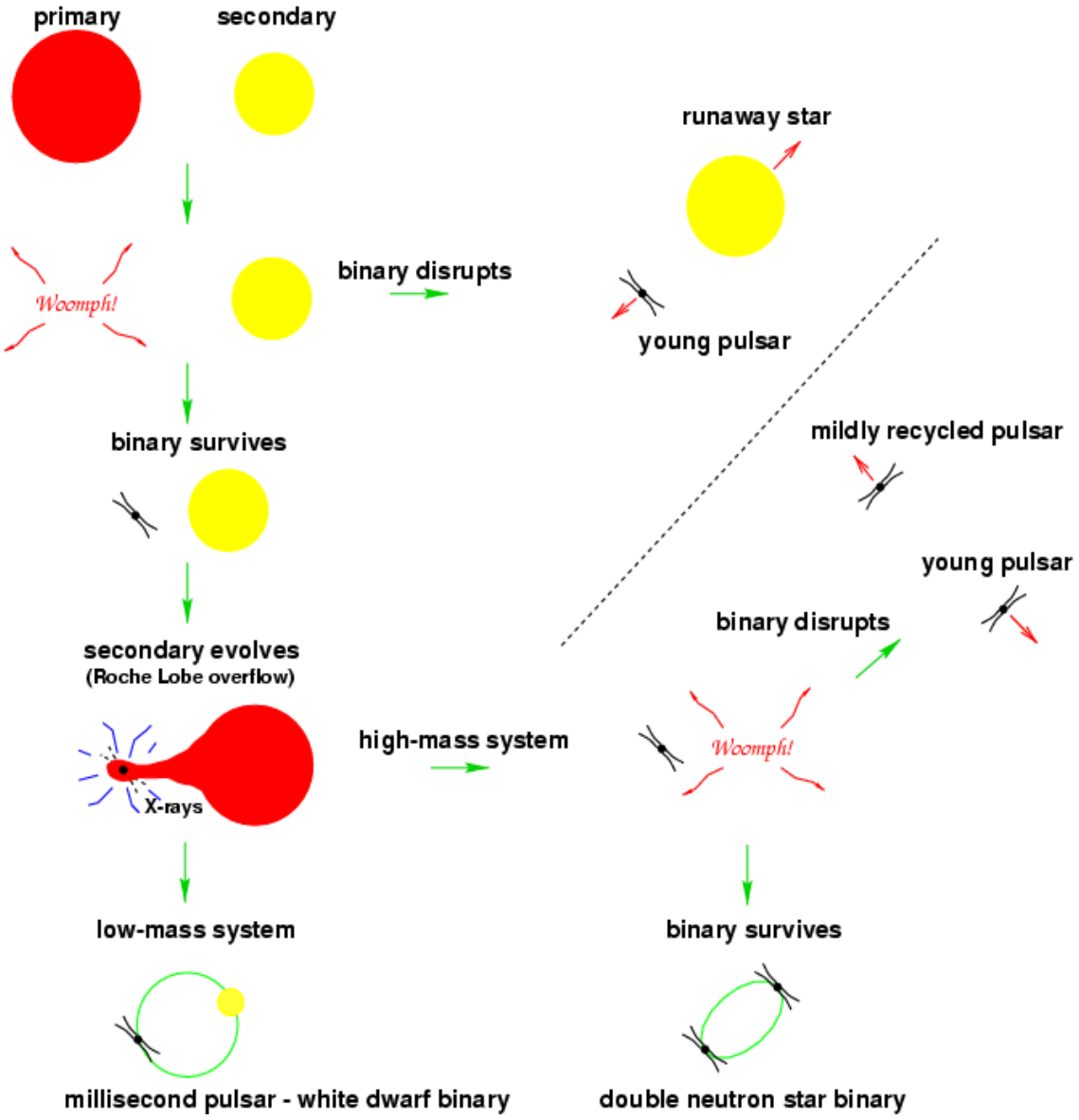

Figure 2.2: A cartoon with various evolutionary paths of binary systems hosting a pulsar

2.1 Binary Millisecond Pulsars in Galactic GCs

Despite the large difference in total mass between the disk of the Galaxy and the Galactic GC system (up to a factor 10^3), the percentage of fast rotating pulsar in binary systems found in the latter is very higher. MSPs in GCs show spin periods in the range $1.3 \div 30\,\mathrm{ms}$,

slowdown rates $\dot{P} \lesssim 10^{19}\,\mathrm{s/s}$ and a lower magnetic field, respect to "normal" radio pulsars, $B \sim 10^8\ gauss$. The high probability of disruption of a binary systems after a supernova explosion, explain why we expect only a low percentage of recycled millisecond pulsars respect to the whole pulsar population. In fact only the 10% of the known 1800 radio pulsars are radio MSPs.

Is not surprising, that MSP are overabundant in GCs respect to Galactic field, since in the Galactic Disk, MSPs can only form through the evolution of primordial binaries, and only if the binary survives to the supernova explosion which lead to the neutron star formation. On the other hand, the extremely high stellar density in the core of GCs, relative to most of the rest of the Galaxy, favors the formation of several different binary systems, suitable for the recycling of NSs (e.g. Davies & Hansen, 1998).

More than 130 MSP have been found in 25 globular cluster up today, their mean observational radio characteristics being:

- very short rotational periods: $P \sim 1.3 \div 20\,\mathrm{ms}$;
- magnetic field in the range $10^{8\div9}\ gauss$:
- an high fraction of binary ($\gtrsim 70\%$ compared to the $\sim 3\%$ of the normal pulsars);
- large characteristic ages $\tau_c \sim 10^{9\div10}\,\mathrm{yr}$
- large characteristic ages of the companions, $T \sim 10^{10}\ yr$, tipical of the old stellar population in globular clusters

In opposition, globular clusters host only $2 \div 3$ "normal" pulsar, i.e. single pulsar with a spin period P$\sim 1sec$ and a magnetic field two order of magnitude higher $B \sim 10^{10\div11}\ gauss$. An up -to-date list of millisecond pulsars propertis in galactic globular clusters is manteined in the P. Freire's web page [1].

As already known from more than 30 years, globular clusters also host a large population of X-ray sources, respect to the galactic field: with the new millenium, the study of X-ray sources in globular clusters received a new boost with the launch of the

[1] http://www.naic.edu/ pfreire/GCpsr.html

new generation of instruments on board *Chandra* and *XMM* satellites, especially with the capability of *Chandra* to detect low -luminosity ($L_x \simeq 10^{30}\ erg\ s^{-1}$) X-ray sources in a large numbers: the high spatial resolution of *Chandra* also permits to distinguish the emission of single sources with an accuracy of ($0''.1 \div 0''.2$) : see for example the large number of sources discovered in 47 Tuc, NGC6266, NGC288, Ter 5 (Grindlay et al, 2001b; Grindlay et al., 2002; D'Amico et al., 2002; Pooley at al., 2003; Kong et al., 2006; Heinke et al., 2006); if most of this sources should be Cataclismyc Variables and quiescent low-mass X-ray binary, MSPs also contributes to the total numbers of X-ray sources, as demonstred from Grindlay et al. (2001b) that identefied 19 X-ray counterparts of radio MSPs in the globular cluster 47 Tuc. Theoretical works in the last 20 years shows that the encounter frequency Γ (i.e. the number of encounters between single stars in a globular cluster) can be defined as $\Gamma \propto \rho_0^{3/2} r_c^2$ (Hut & Verbunt, 1983; Verbunt, 2006; Pooley & Hut, 2006), being ρ_0 the central density of the cluster and r_c its core radius. The strong correlation between the encounter frequency and the X-ray sources provide a clear evidence that low-luminosity X-ray sources in globular clusters are formed through stellar encounters. Fig.2.3 shows this correlation; we noticed that cluster lying in the upper-right corner of the figure are the cluster with the larger population of MSPs, strongly supporting the idea that also this sources in globular clusters are formed through stellar encounters.

The high accuracy in the determination of the radio MSPs, combined with the detection of large numbers of cataclysmic variable, active binary with both *Chandra* and HST has allowed to place on a common astrometric frame, good to $\lesssim 0''.1$, the radio, optical and X-ray data.

2.2 Optical Counterparts of Binary Millisecond Pulsars in Galactic GCs

As discussed above, more than 130 MSPs, half of all those known, have been found in radio surveys of GCs, in which the high stellar densities and interaction rates cause large numbers of neutron stars to be spun-up to millisecond periods via binary production and subsequent accretion onto the compact object. Studies of these objects therefore

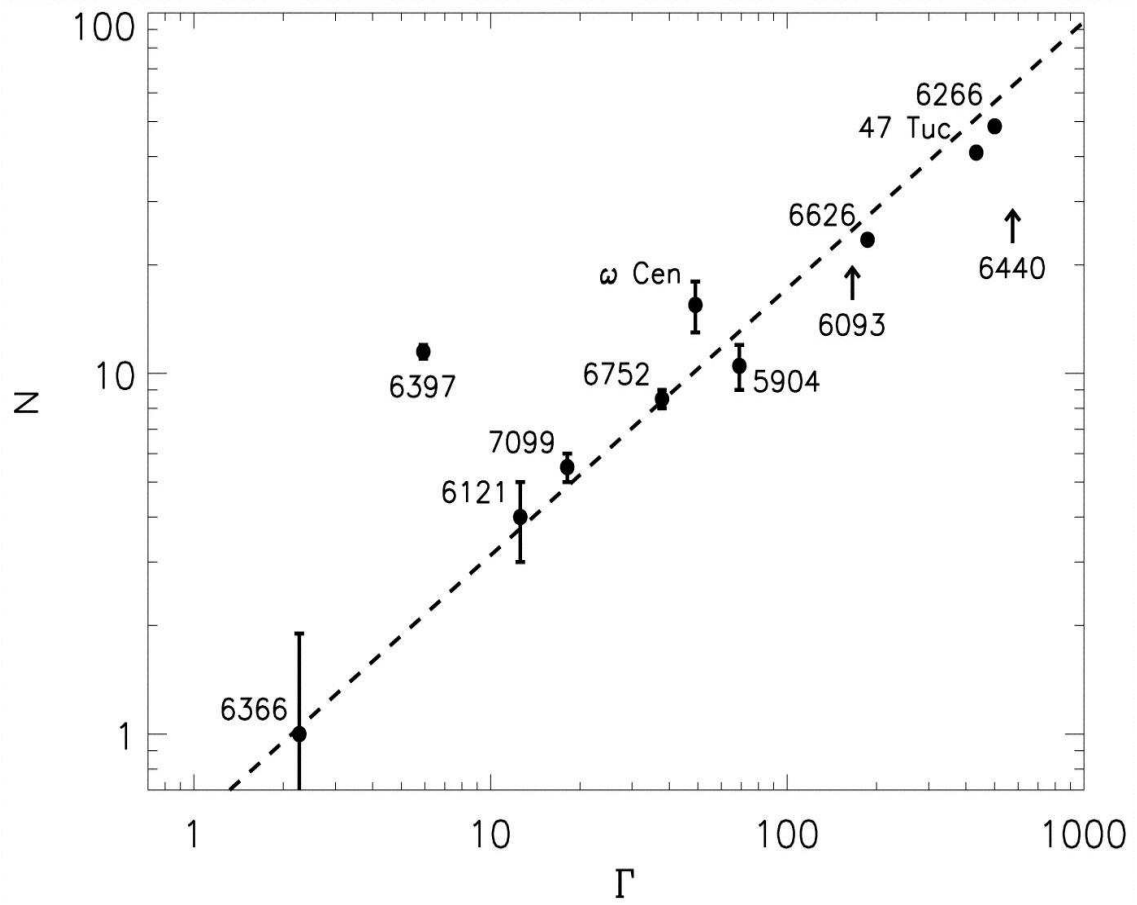

Figure 2.3: Number of observed cluster X-Ray sources with $L_x \gtrsim 4 \times 10^{30}\, erg/sec$ versus the encounter rate Γ. The N_x error bars are due to the uncertanties in the background sources counts. The arrows indicates globular clusters for which the *Chandra* observation did not reach the required sensitivity

offer insight into the formation and evolution of neutron star binaries (e.g. Rasio Pfahl & Rappaport, 2000) and the frequency of stellar interactions in the dense cores of clusters, and sample different evolutionary channels compared to the disk population.

Recent improvements in the radio telescopes sensitivity have resulted in a dramatic increase in the number of MSPs detected in GCs. For example, the 11 known MSPs in the GC 47 Tuc (Manchester et al., 1991; Robinson et al., 1995) have been recently increased to 24 (Camilo et al., 2000; Lorimer et al., 2003; Bogdanov et al., 2005), whereas a surprisingly large population of 33 MSPs has been recently discovered in Terzan 5, (Ransom et al., 2005; Hessels, 2006).These results enable studies of the cluster's

gravitational potential well (Freire et al., 2001a) and of the intra-cluster medium (Freire et al., 2001b).

Binary MSPs in clusters offer the crucial advantages of studying these systems at well-determined distance, age, metallicity and reddening. Accurate distances are particularly important for reducing uncertainties in luminosity, and making reliable cluster-to-cluster and cluster-to-field comparisons.

The optical detection of the companion to a binary MSP in a GC proved particularly helpful in assessing the origin and the evolution of the binary, besides supporting its cluster membership (see, e.g., Edmonds et al., 2001; Ferraro et al., 2001a; Edmonds et al., 2002). In fact, unlike the systems in the galactic field, the age, metallicity, extinction, distance and hence intrinsic luminosity and radius of the MSP companion can be estimated from the parent cluster parameters.

Moreover binary MSPs can be very helpful for studying the dynamical interactions that can take place in a GC. Besides the investigation of radius, mass and cooling age of the companion, the observation of the degree of modulation of the optical flux from the companion at the orbital period will allow to measure heating effects of the pulsar impinging on the companion surface, helping in clarifying if it will be evaporated by the pulsar.

Despite these promising goals, observational progresses in detecting optical counterparts of cluster binary MSPs are quite slow (up to now only six of such counterparts were identified), mainly because of the high spatial resolution needed and sensitivity limitations.

2.2.1 Optical companion of MSPs in 47 Tuc

The first two detections of MSP companion in a GC was $U_{\rm opt}$, the companion to PSR J0024−7203U and the faint and blue source W29, the companion to the MSP PSR J0024−7204W, both in 47 Tuc (Edmonds et al., 2001, 2002); the position of $U_{\rm opt}$ in a Color Magnitude Diagram and the comparison with theoretical models reveals that this star is a low-mass ($\lesssim 0.17 M_{\odot}$) Helium White Dwarf. This is the more common by product of the recycling process, in which the evolution of a normal low mass star out to

the MS start the transfer of mass and angular momentum onto the NS surface. At the end of the mass transfer the companion of the MSP have lost the external envelope, leaving only the degenerate He core.

47 Tuc also host the second optical companion of a MSP in a GC, the very faint ($V = 22.3$, $V - I = 0.7$) and blue source W29, identified as the companion to the MSP PSR J0024−7204W. This object is most peculiar and intriguing than $U_{\rm opt}$. The star shows a large amplitude (60%-70%) sinusoidal variation in both V and I. The phase dependence of the intensity and color implies that heating of a tidally locked companion causes the observed variations: the radiation flux coming from the pulsar heat the surface of the companion, that once per orbit, shows the hotter and brighter side to the observer. The eclipsing nature of PSR J0024−7204W, combined with the relatively large companion mass ($M_c > 0.13 M_\odot$) and the companion's position in the CMD, are completely inconsistent both with the WD characteristics and with the normal MS population of the cluster. Combining these evidences with the X-ray eclipses observed by Chandra (Grindlay et al., 2002), the authors conclude that this system may be composed by a MSP and a very light MS star.

2.2.2 The White Dwarf orbiting PSR B1620-26 in M4

Another white dwarf has been found orbiting around PSR B1620-26 in the Globular Cluster M4 (Sigurdsson et al., 2003). In this case, the comparison with cooling traks of white dwarfs (Wood, 1995), suggest that the companion of PSR B1620-26 is a little bit more massive Carbon-Oxigen WD, with mass $M_c \simeq 0.28\,M_\odot/\sin i$ as estimated from the radio timing or $M_c \simeq 0.35\,M_\odot$ as derived from the position of the star in the CMD. Carbon Oxigen white dwarf are quite rare as companion of MSP in GC, and just few MSP are suspected from radio timing measurement to have such object as companion. A lower, $M \simeq 0.2 M_\odot$ He-WD is the preferred by-products of the recycling process. Some peculiar characteristics of this system has been found after accurate radio timing. The pulsar possesses an anomalously large second time derivate of the rotational period (seven order of magnitude higher than expected from the pulsar spin down and of the wrong sign)and further radio observations reveled the third and fourth derivatives of the

pulsar period as well as a secular change in the projected semimajor axis of the inner binary. On the basis of these contraints, Sigurdsson et al. (2003) proposed a model in which a third body (=a planet) is responsable for the observed time varying acceleration.

2.2.3 The tidally deformed companion to the PSR J1740-5340 in NGC6397

The most peculiar optical companion of MSP in GC is the companion of the eclipsing millisecon pulsar PSR J1740-5340 in the globular cluster NGC6397, found by Ferraro et al. (2001b). This object turn out to be a bright ($V \simeq 16.7$) red ($V - I \simeq 0.9$) and variable star (see Fig 1 of Ferraro et al. 2001b). The optical variability of this star nicely correlates with the orbital period of the binary systems ($P_{orb} \simeq 1.35\ days$), but the characteristic of the light curve are unprecedented for a MSP companion, being the clear signature of a tidally deformed star. In fact, as shown in Fig2.4, the light curve, both in U and in H_α filters is characterized by two maxima at orbital phases 0 and 0.5. Hereafter in this thesis we locate at phase 0 and 0.5 the two quadratures and at phases 0.25 and 0.75 the two conjunctions. Thus at phase 0.25 (the superior conjunction of the companion star) we see the face of the companion heated from the radiation coming from the pulsar. The maxima at the quadratures indicates that the companion is tidally deformed and has filling its Roche Lobe. In these phases the companions shows to the observer the major axis of its ellipse, resulting brighter. The matter overflowing the Roche Lobe is also responsable of the eclipse of the radio signal observed at the superior conjunction of the pulsar, when the companion is located between the pulsar and the observer.

A fascinating possibility is that PSR J1740-5340 is a newborn MSP, the first one observed just after the end of the process of recycling. In this case (Burderi D'Antona & Burgay, 2002), the companion star could have been originally a MS star of $M \leq 1 M_\odot$ whose evolution triggered mass transfer toward the compact companion, spinning it up to millisecond periods. Irregularities in the mass transfer rate from the companion, $\dot{M}_c$ are common in the evolution of these systems (e.g., Tauris Savonije 1999): even a short decreasing of $\dot{M}_c$ can have easily allowed PSR J1740-5340 (having a magnetic field $B_p \lesssim 10^9 gauss$ and a rotational period 3.65 ms) to become source of relativistic

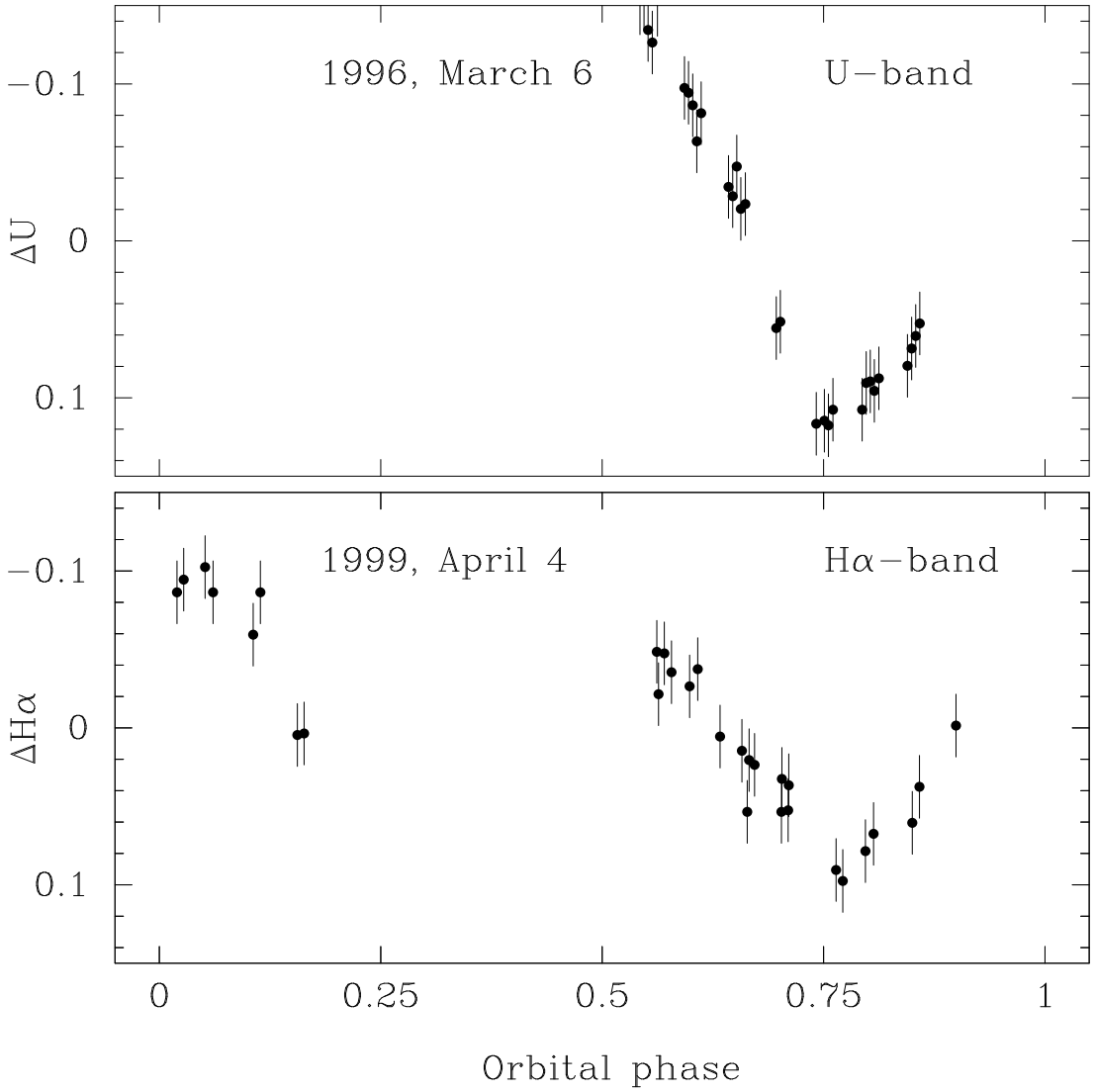

Figure 2.4: Light curves of the companion to the pulsar PSR J1740-5340, as a function of the pulsar orbital period (Ferraro et al., 2001b). The light curve in different band, and taken in different epochs, plotted versus the phase. The maxima at the quadratures an the minima at the conjunctions are the clear indication of ellipsodal modulation due to a tidally deformed star.

particles and magnetodipole emission, whose pressure (1) first swept the environment of the NSs, allowing coherent radio emission to be switched on (Shvartsman, 1970), and (2) then kept on expelling the matter overflowing from the Roche lobe of the companion (Ruderman Shaham & Tavani, 1989). For a wide enough binary system (as is the case of PSR J1740-5340), once the radio pulsar has been switched on, any

subsequent restoration of the original $\dot{M}_c$ cannot quench the radio emission (Burderi et al. 2001). In this case, we have now a donor star still losing matter from its Roche lobe at $\dot{M}_c \gtrsim 5 \times 10^{-11} M_\odot yr^{-1}$(D'Amico et al. 2001c; a high mass-loss rate, difficult to explain in the model of a bloated star). At the same time, accretion on the NS is inhibited because of the pressure exerted by the pulsar on the infalling matter. This strong interaction between the MSP flux and the plasma wind would explain also the irregularities seen in the radio signals from PSR J1740-5340, sometimes showing the presence of ionized matter along the line of sight even when the pulsar is between the companion star and the observer. The characteristic age of PSR J1740-5340 ($3.5 \times 10^8 yr$) would indicate that it is a young MSP, further supporting this scenario. If the companion star will continue releasing matter at the present inferred rate, PSR J1740-5340 is not a candidate for becoming an isolated pulsar. When the companion star will have shrunk well inside its Roche lobe, the system will probably end up as MSP + WD (or a light nondegenerate companion). If alternatively it will undergo a significant increasing of $\dot{M}_c$, the condition for the accretion could be reestablished and PSR J1740-5340 would probably appear again as a low-mass X-ray binary or as a soft X-ray transient (Campana et al., 1998).

In the following chapters we will present the properties of the other two millisecond pulsars companions discovered in globular clusters, the Helium white dwarf orbiting the MSP PSR 1911-5958A in NGC 6752 and the second case of a tidally deformed star orbiting an eclipsing millisecond pulsar, PSR J1701-3006B in NGC6266

2.3 Search for optical counterparts: a methodological approach

As previously discussed, mass segregation and high densities favor the formation of MSPs in the globular clusters cores; as a consequence identifications optical emission from the MSP companions are quite problematic. Indeed the normal companions to MSPs are white dwarfs (WDs), and/or light, nearly exhausted, main sequence (MS) stars. Such sources are intrinsically faint; this physical characteristic, connected to the high crowding

conditions, typical of the clusters cores, tends to to make the identifications difficult.

Another delicate step in the detection of optical counterparts to MSPs companions is the necessity of high accurate absolute position for the optical data. In fact, while the position of a MSP is known with extremely high precision from the radio timing measurements, the absolute astrometry for optical data is a complicate task. This is even more complicate in the central region of a cluster, where usually there are not primary astrometric standard stars. Then the small field of view of the high resolution cameras, as the HST-ACS or HST-WFPC2, requires to combine high-resolution images (which can properly sample the most crowded regions of the cluster core) with wide-field images, which allow to observe an appropriate number of primary astrometric standard stars in the cluster adjacent regions. Thus by cross-correlating the wide field image catalog with the astrometric one (e.g. the Guide Star Catalog – GSCII, available at `http://www.gsss.stsci.edu/gsc/gsc2/GSC2home.htm`) it is possible to get accurate absolute positions with rms residuals of the order of $\sim 0\,\overset{''}{.}\,3 \div 0\,\overset{''}{.}\,4$ both in RA and Dec.

In all the astrometric analysis shown in the following chapters, HST data have been cross-correlated with data acquired by the Wide Field Imager (WFI) at the ESO 2.2m telescope (at European Southern Observatory, La Silla, Chile). The images produced by this telescope consist of a mosaic of 8 chips (see Fig.2.5), each with a field of view of $8' \times 16'$, giving a global field of view of $33' \times 34'$. WFI observation of clusters used in this thesis were performed in such a way to image the central part of the observed cluster in one chip.

The small field of view (FoV$\sim 2'.5$ on the side) of the high resolution HST-WFPC2 images is normally entirely contained within the FoV of one WFI chip, which imaged central part of the cluster (see Fig.2.5). Thus all the bright stars in the WFI catalog, lying also in the high-resolution FoV, can be used as *secondary astrometric standards* in order to properly find an astrometric solution of the WFPC2 catalog. Note that at the end of the procedure the two catalogs (high-resolution and wide-field) have a fully homogeneous absolute coordinate system.

In order to identify the companion to a binary MSP, all stars lying in a 3σ error box

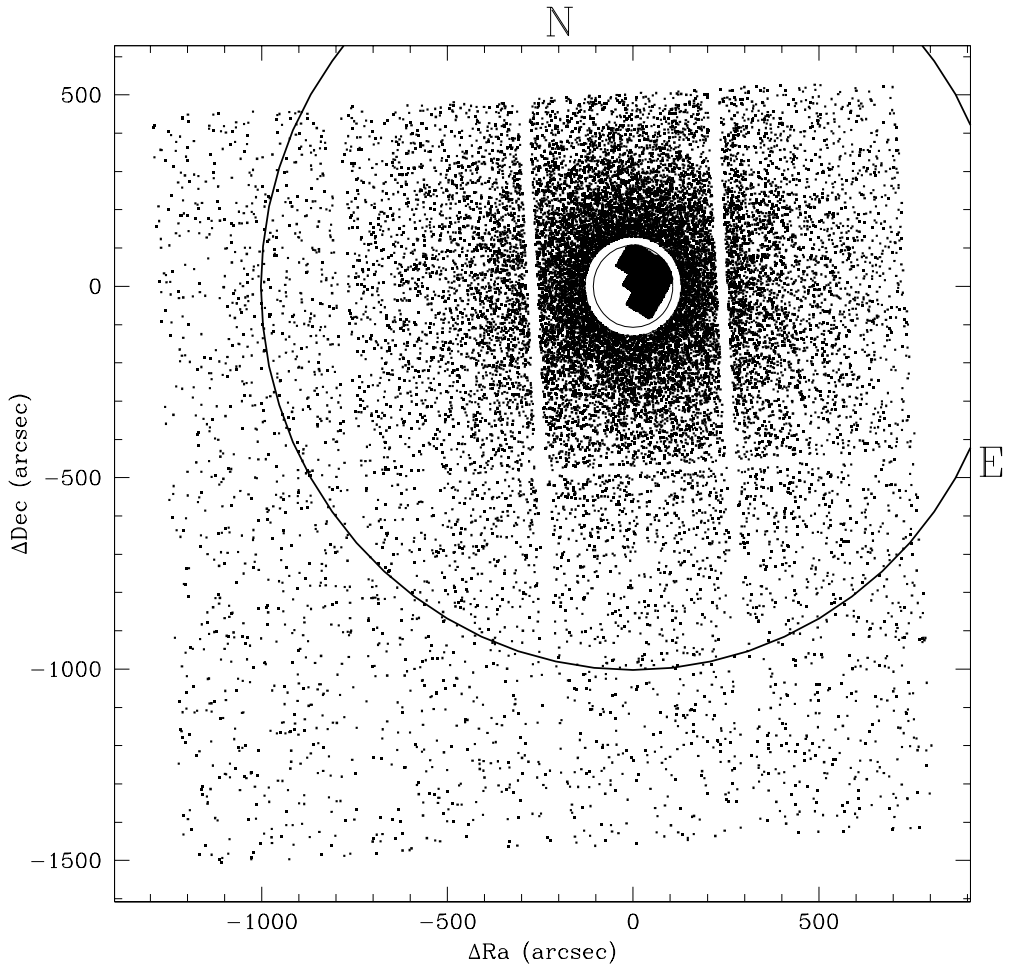

Figure 2.5: Computed map of the NGC 6752: HST and WFI FoV. The black circular line has a radius of 16′.67 and it is centered on the cluster center of gravity (C_{grav}).

are accurately analyzed: as already quoted above, the companions to MSPs are aspected to be WD, hence they should show a blue excess and lays to the left of the cluster MS in the CMD (see for instance Fig. 3.4).

MSP companions often show a modulation in their luminosity. When analyzed, light curves of the companions nicely correlate with MSP orbital period (see Figs. 2.4 & 4.5) and can reveal the presence of heating effects on the companion surface, or, as in the case of the COM J1740−5340 (Ferraro et al., 2001b), and COM J1701-3006B (Cocozza et al., 2008), the occurrence of tidal distortion. The detection of variability in the emission

of candidate companion, correlated with the orbital period of the MPS, not only further confirms the identification, but also allow to make some predictions on the evolution of the binary system.

Chapter 3

The puzzling properties of the Helium White Dwarf orbiting the Millisecond Pulsar A in the Globular Clusters NGC 6752

3.1 Introduction

Although NGC 6752 is one of the nearest clusters, there is no consensus in the literature on its dynamical status. It was initially classified as a post-core collapse (PCC) by Djorgovski & King (1986) and Auriere & Ortolani (1989). Later Lugger Cohn & Grindlay (1995) argued that the radial profile was not inconsistent with a King model.

Recently, observations of $|\dot{P}/P|$ and location of five millisecond pulsars (see Fig. 3.1) in NGC 6752 (D'Amico et al., 2002) have suggested a surprisingly high mass-to-light ratio $\mathcal{M}/\mathcal{L}_V$ in its core and the occurrence of non thermal dynamics in the inner regions (see Colpi Possenti & Gualandris, 2002). The determination of $\mathcal{M}/\mathcal{L}_V$ by D'Amico et al. relied on results of pulsar timing and published optical data derived from medium resolution ground based observation only. Taking advantage from new optical data, Ferraro at al. (2003) re-examined this measurement, discussing the possible origin and the consequences of the observed values of $|\dot{P}/P|$ at some length.

The five MSPs hosted in NGC 6752 have been discovered on 1999 October 17 during a search for MSPs in galactic GCs in progress at the Parkes Radiotelescope (D'Amico et al., 2001a). Three of them are located in the central regions of the globular, as

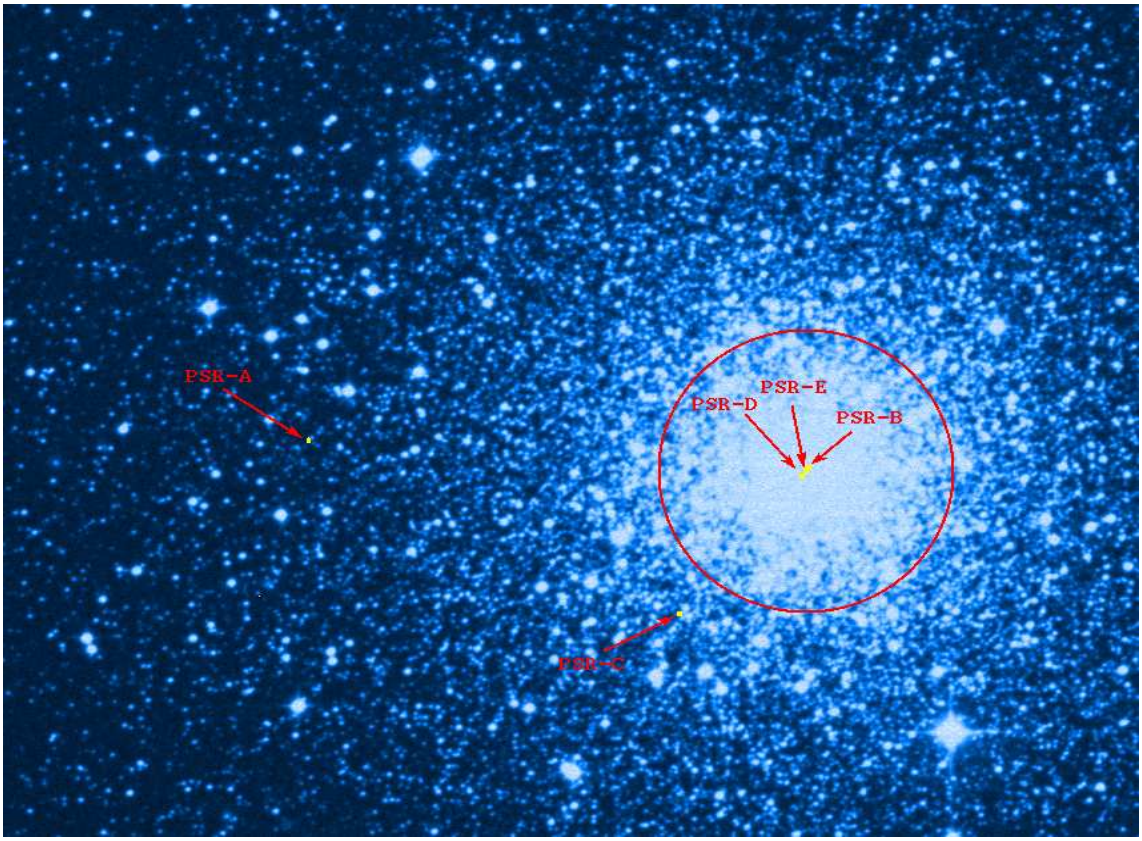

Figure 3.1: Positions of the 5 MSP (indicated by arrows) found in NGC 6752 (D'Amico et al., 2002), superposed on an optical image of the cluster. The circle indicates the half-mass radius region (r_{rh}=115").

normally expected on the basis of the mass segregation in a cluster. The other two are the most external MSPs bounded to a GC ever detected until now. PSR J1911−5958A, in particular, is a binary MSP (the only binary MSP found in this cluster) and has a position $\sim 6'.4$ away from the cluster optical center: indeed PSR J1911−5958A is the most off-centered pulsar among the whole sample of MSPs whose position in the respective cluster is known, and it suggests that this object might be the result of strong interactions occurred in the cluster core.

3.2 The dynamical status of NGC 6752

Ferraro et al. 2003 also found a significant deviation of the star number density profile from a canonical King model, interpreting this fact as a clear indication that the innermost

TABLE 1

MEASURED AND DERIVED PARAMETERS FOR FIVE MILLISECOND PULSARS IN NGC 6752

Parameter	PSR A	PSR B	PSR C	PSR D	PSR E
Name	J1911−5958A	J1910−5959B	J1911−6000C	J1910−5959D	J1910−5959E
R.A. (J2000)	19 11 42.7562(2)	19 10 52.050(4)	19 11 05.5561(7)	19 10 52.417(2)	19 10 52.155(2)
Decl. (J2000)	−59 58 26.900(2)	−59 59 00.83(3)	−60 00 59.680(7)	−59 59 05.45(2)	−59 59 02.09(2)
P (ms)	3.2661865707911(5)	8.35779850080(3)	5.277326932317(4)	9.03528524779(2)	4.571765939765(7)
$\dot{P}$	$3.07(10) \times 10^{-21}$	$-7.99(5) \times 10^{-19}$	$2.2(7) \times 10^{-21}$	$9.63(3) \times 10^{-19}$	$-4.37(1) \times 10^{-19}$
Epoch (MJD)	51920.0	52000.0	51910.0	51910.0	51910.0
DM (cm $^{-3}$pc)	33.68(1)	33.28(4)	33.21(4)	33.32(5)	33.29(5)
P_{orb} (days)	0.837113476(1)	...	...	...	...
$a_p \sin i/c$ (s)	1.206045(2)	...	...	...	...
T_{asc} (MJD)	51919.2064780(3)	...	...	...	...
Eccentricity	$<10^{-5}$	...	...	...	...
M_c ($M_\odot$)	>0.19	...	...	...	...
MJD Range	51710–52200	51745–52202	51710–52201	51744–52197	51744–52201
Number of TOAs	74	27	94	38	38
Residual (μs)	10	83	55	55	60
S_{1400} (mJy)	0.22	0.06	0.30	0.07	0.09
Offset[a] (arcmin)	6.39	0.10	2.70	0.19	0.13

Figure 3.2: Derived parameters and positions of the 5 MSP found in NGC 6752 (D'Amico et al., 2002).

region of NGC 6752 has experienced (or is experiencing) a collapse phase. Unfortunately, no similarly unambiguous signature is available for differentiating the in- and post-core collapse state (Meylan & Heggie, 1997). However, in favorable cases the phase of the collapse can be evaluated from indirect evidence.

This results support the earlier suggestions of post-core collapse bounce (Auriere & Ortolani, 1989). Post-core collapse clusters are expected to undergo large amplitude oscillations in core size due to the gravothermal instability of collisional systems (e.g. Cohn et al., 1991). The oscillating core spends most of the time at near maximum size and a radial extension of 0.11 pc is consistent with the maximum radius of the core predicted by the models of post-core collapse bounce. The parameter most commonly used in theoretical studies is the ratio of core radius to half-mass radius, r_c/r_h. Using the value of $r_c = 5\,\overset{''}{.}2$ and the half-mass radius of 115" from Trager King & Djorgovski (1995), this ratio results for NGC 6752 $r_c/r_h = 0.045$. For comparison, the multi-mass Fokker-Planck models for the post-collapse evolution of M15 presented by Grabhorn et al. (1992, see

their Fig. 5) reach a comparable value of $r_c/r_h = 0.034$ during the maximally expanded state of the most extreme core bounces. The inclusion of primordial binaries in Monte Carlo simulations by Fregeau et al. (2003) results in an even wider range of predicted r_c/r_h in the post-collapse phase.

Furthermore, there is an intermediate region in the composite density profile of NGC 6752 which is well represented by a power law profile with a slope $\alpha \sim -1$, compatible with the steepness predicted by single mass models of expanding bouncing cores (Lugger Cohn & Grindlay, 1995).

It is also worth noting that NGC 6752 has apparently retained a substantial primordial binary population (Rubenstein & Bailyn, 1997); these binaries may play an important role in supporting the core and delaying the core-collapse event. In this respect, Ferraro et al. (1999a) have suggested that some species originated from binary evolution could be used as possible tracers of the cluster dynamical evolution. In particular, the large BSS population recently found in M80 by Ferraro et al. (1999a) might be the signature of a transient dynamical state, during which stellar interactions are delaying the core-collapse process leading to an exceptionally large population of *collisional*-BSS. On the other hand the BSS population found in the central region of NGC 6752 is small (Sabbi et al., 2004) perhaps indicating that NGC 6752 is in a different dynamical evolutionary state than M80: maybe the binary population in NGC 6752 has not been "burned out" producing collisional BSS while that in M80 has.

3.3 The interpretation of the MSPs accelerations

NGC 6752 hosts 5 known millisecond pulsars (D'Amico et al., 2001a, 2002, see Fig. 3.3). The positions in the plane of the sky of three of them (PSRs B, D and E, all isolated pulsars) are close to the cluster center, as expected on the basis of mass segregation in the cluster, but PSR-B and E show large *negative* values of $\dot{P}$, implying that the pulsars are experiencing an acceleration with a line-of-sight component a_l directed toward the observer and a magnitude significantly larger than the positive component of $\dot{P}$ due to the intrinsic pulsar spin-down (see e.g. Phinney, 1992).

What is the origin of such acceleration? Given the location of NGC 6752 in the galactic halo and knowing its proper motion (Dinescu Girard & van Altena, 1999), it is possible to calculate the contributions to $\dot{P}$ due to centrifugal acceleration, differential galactic rotation and vertical acceleration in the Galactic potential, all of them resulting negligible (D'Amico et al., 2002). Hence, the remaining plausible explanations of the observed negative $\dot{P}$ are the accelerating effect of the cluster gravitational potential well or the presence of some close perturbator(s) exerting a gravitational pull onto the pulsars.

3.3.1 Case (i): Overall effect of the GC potential well

The hypothesis that the line-of-sight acceleration of the MSPs with negative $\dot{P}$ is dominated by the cluster gravitational potential has been routinely applied to many globulars. In particular from this assumption a lower limit to the mean projected mass-to-light ratio in the V-band $\mathcal{M}/\mathcal{L}_V$ in the central region of M15 (Phinney, 1992) and 47 Tucanae (Freire et al., 2003), yielded $\mathcal{M}/\mathcal{L}_V \gtrsim 3$ and $\gtrsim 0.7$ respectively. Following (Phinney, 1992), a lower limit to $\mathcal{M}/\mathcal{L}_\mathcal{V}$ in the inner regions of NGC 6752 is given by

$$\left|\frac{\dot{P}}{P}(\theta_\perp)\right| < \left|\frac{a_{l,max}(\theta_\perp)}{c}\right| \simeq$$
$$\simeq 1.1\frac{G}{c}\frac{M_{cyl}(<\theta_\perp)}{\pi D^2\theta_\perp^2} = 5.1\times10^{-18}\frac{\mathcal{M}}{\mathcal{L}_V}\left(\frac{\Sigma_V(<\theta_\perp)}{10^4\ \mathrm{L_{V\odot}pc^{-2}}}\right)\mathrm{s}^{-1},$$

where $\Sigma_V(<\theta_\perp)$ is the mean surface brightness within a line of sight subtended by an angle $\theta_\perp$ with respect to the cluster center and $M_{cyl}(<\theta_\perp)$ is the mass enclosed in the cylindrical volume of radius $R_\perp = D\theta_\perp$. This equation holds to within $\sim 10\%$ in all plausible cluster models and is independent of cluster distance, except for the effects of extinction. Since $E(B-V)$ is very small for NGC 6752 (= 0.04 according to Harris, 1996) the latter is a negligible affect for this cluster.

Using the observed $\dot{P}/P$ of PSR-B and PSR-E (D'Amico et al., 2002), combined with the accurate determinations of $C_{\rm grav}$ (the cluster center of gravity) and $\Sigma_V(<r)$ (the mean surface brightness radial profile), it turns out that $\mathcal{M}/\mathcal{L}_V \gtrsim 6 \div 7$ for the case of NGC 6752.

D'Amico et al. (2002) obtained a slightly larger $\mathcal{M}/\mathcal{L}_V \gtrsim 10$ using published values of $C_{\rm grav}$ and $\Sigma_V(<r)$ derived from medium resolution ground based observations only.

The difference between the two estimates is mainly due to the refined new position of the cluster center of gravity.

Despite a residual uncertainty $\sim 0''.7$ on $C_{\rm grav}$, under the hypothesis that the line-of-sight acceleration of PSR-B and PSR-E are entirely due to the cluster gravitational potential, a lower limit of $\mathcal{M}/\mathcal{L}_V \gtrsim 5.5$ can be firmly established. It is obtained assuming that the two millisecond pulsars were just symmetrically located (and hence at the minimum projected distance) with respect to the actual center of gravity.

The sample of the core collapsed clusters shows typical values of the projected central mass-to-light ratio in the interval $2 \div 3.5$ (Pryor & Meylan, 1993), although larger $\mathcal{M}/\mathcal{L}$ ratios can be obtained when a Fokker–Planck model fit is used (e.g. the case of M15 Dull et al., 1997, 2003). If we take $\mathcal{M}/\mathcal{L}_V \gtrsim 3$, the expected total mass located within the inner $r_{\perp,B} = 0.08$ pc of NGC 6752 (equivalent to the projected displacement of PSR-B from $C_{\rm grav}$) would be $\sim 1200 \div 2000\,{\rm M}_\odot$. On the other hand, the observed $\mathcal{M}/\mathcal{L}_V \sim 6 \div 7$ implies the existence of further $\sim 1500 \div 2000\,{\rm M}_\odot$ of low-luminosity matter segregated inside the projected radius $r_{\perp,B}$. This extra amount of mass could be constituted by a relatively massive black hole, like the $\sim 1700^{+2700}_{-1700}\,{\rm M}_\odot$ black hole in the center of the globular cluster M15 recently proposed by (Gerssen et al., 2003).

Results presented from Sabbi et al. (2004) shows that there are significant differences in the kinematics and mass distributions of the central regions of M15 and NGC 6752 (we note here that because the distance to NGC 6752 is less than half that to M15, its inner core is more easily studied):

- HST imaging of M15 (Guhathakurta et al. 1996 — WFPC2; Sosin & King 1997 — FOC) shows no evidence for a compact core, at variance with the observations of the core of NGC 6752;

- The derived stellar density profiles of M15 have power law slopes consistent with $\alpha = -0.75$ (expected from single mass models with a dominant central black hole, Lugger Cohn & Grindlay (1995)). If a $\gtrsim 10^3\,{\rm M}_\odot$ black hole resides in the inner region of NGC 6752, its gravitational influence would extend more than ~ 2" from the center of the cluster and probably produce a central power-law cusp, which in

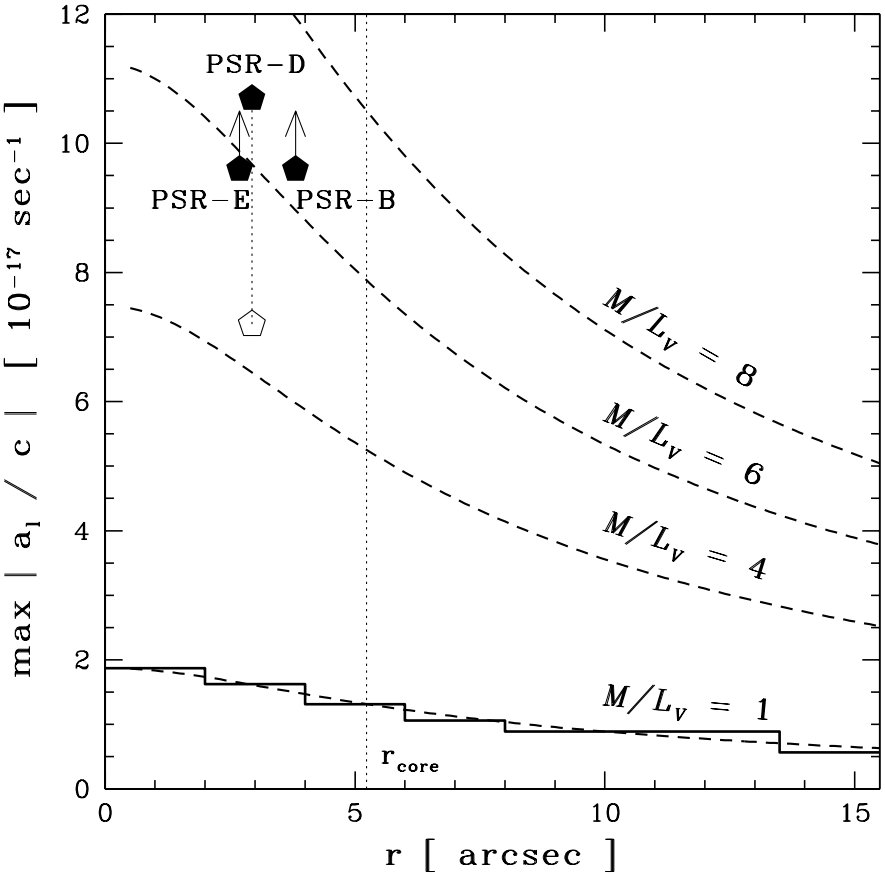

Figure 3.3: Maximum line-of-sight acceleration $|a_{l_{max}}/c| = |\dot{P}/P|$ versus radial offset with respect to the center of NGC 6752. The histogram represents the prediction based on the star density assuming a unity mass-to-light ratio. The dashed lines are analytical fits to the optical observations, labeled according to the adopted mass-to-light ratio. The measured values of $\dot{P}/P$ (filled pentagons, D'Amico et al., 2002) in the two MSPs with negative $\dot{P}$ (PSR-B and E) can be reproduced only for $\mathcal{M}/\mathcal{L}_V \gtrsim 6 \div 7$. The open pentagons show the best guess for the range of maximum $|a_l/c|$ for PSR-D: the upper value is calculated assuming a negligible intrinsic positive $\dot{P}_{sd}$; the lower value is estimated taking into account intrinsic $\dot{P}_{sd}$ from the observed scaling between X-ray luminosity and spin-down power for MSPs (see D'Amico et al., 2002, and reference therein). Given the relative large uncertainty, the value of $|a_l/c|$ it is not further taken into account in the discussion.

NGC6752 is not observed.

A very high $\mathcal{M}/\mathcal{L}_V \sim 6 \div 7$ could be also due to central concentration of dark remnants of stellar evolution like neutron stars (NSs) and heavy $\sim 1.0\,\mathrm{M}_\odot$ white dwarfs (WDs) (as also proposed for M15 by Dull et al., 1997, 2003; Baumgardt et al., 2003). In this case, one can constrain the initial mass function (IMF) and/or the neutron star retention fraction $f_{\rm ret}$ in NGC 6752.

On the basis of the current population of turn-off stars (in the mass interval $0.6 \div 0.8\,\mathrm{M}_\odot$), the estimated number of upper main sequence initially present in NGC 6752 is ~ 4000 (D'Amico et al., 2002). This assumes a Salpeter-like IMF ($\alpha_{IMF} = 2.35$ which is consistent with that measured by Ferraro et al., 1997b). If the low-luminosity matter observed in the central $0.08\,\mathrm{pc}$ were entirely due to ≈ 1300 NSs of $1.4\,\mathrm{M}_\odot$, then $f_{\rm ret} \sim 30\%$ (a reasonable value for collapsed clusters – Drukier, 1996).

Alternatively, $\mathcal{M}/\mathcal{L}_V \sim 6 \div 7$ can be explained by a Salpeter IMF if $\gtrsim 20\%$ of the total population of heavy $1.0\,\mathrm{M}_\odot$-WDs sank into the NGC 6752 core during the cluster dynamical evolution.

Either scenario must be compared with the observed shape of the star density profile. According to Cohn et al. (1991), during the core collapse phase the surface density slope for the most massive component is expected to be $\alpha = -1.23$ rather than the projected isothermal slope of $\alpha = -1.0$. In the central cusp that forms during core collapse, the surface density slope of a component of stellar mass m is given approximately by:

$$\alpha = -1.89\frac{m}{m_d} + 0.65$$

where m_d is the stellar mass of the dominant component. If the luminosity profile is dominated by turnoff stars of mass $m = 0.8\,\mathrm{M}_\odot$ and has a slope of $\alpha = -1.05$, then the implied mass of the dominant, non luminous component should be $m_d = 0.89\,\mathrm{M}_\odot$, i.e. somewhat more massive than the adopted turnoff mass. This argument does suggest that the central gravitational potential is not likely to be dominated by a large number of neutron stars, but heavy white dwarfs still remain a possibility.

Velocity dispersions provide a further constraint on the nature of the cluster potential

well: the stars dominating the dynamics in the inner part of the cluster should have (see eq. 3.5 of Phinney, 1992) a 1-dimensional central velocity dispersion $\sigma_{v,0} \gtrsim 9 \div 10\,\mathrm{km\,s^{-1}}$. This is compatible both with the very wide published 2σ interval for the $\sigma_{v,0}$ of NGC 6752 ($2.1 \div 9.7\,\mathrm{km\,s^{-1}}$, Dubath Meylan & Mayor, 1997) and with preliminary proper motion measurements of stars in the central part of NGC 6752, which would suggest a significantly higher one-dimension velocity dispersion $\sigma_{v,0} \sim 12\,\mathrm{km\,s^{-1}}$ and the existence of strong velocity anisotropies (Drukier et al., 2003) [1]. Recent Fabry-Perot spectroscopy of single stars in NGC 6752 shows a flat velocity dispersion profile with typical one-dimension velocity dispersion $\sigma \sim 6 \div 7\,\mathrm{km\,s^{-1}}$ within the central $1'$ (Xie et al., 2002). This is also marginally compatible (given the $\sim 10\%$ uncertainty of the formula 3.5 of Phinney, 1992).

3.3.2 Case (ii): Local perturbator(s)

We here explore the alternate possibility that the acceleration imparted to PSR-B and PSR-E are due to some local perturbator.

NGC 6752 is a highly concentrated cluster and its core could host $n_\star \gtrsim 10^6$ stars per cubic pc (assuming an average stellar mass of $\overline{m} \sim 0.5\,M_\odot$), hence close star-star encounters are a viable possibility.

In order to produce the line-of-sight acceleration

$$|a_l| = c|\dot{P}/P| = 2.9 \times 10^{-6}\,\mathrm{cm\,s^{-2}}$$

seen in PSR-B (or PSR-E) a passing-by star of mass $\overline{m}$ must approach the pulsar at

$$s \leq (G\overline{m}|a_l|^{-1})^{1/2} = 0.0015\,\left(\frac{\overline{m}}{0.5\,\mathrm{M_\odot}}\right)^{1/2}\,\mathrm{pc}.$$

An upper limit to the probability of occurrence of a suitable close encounter can be roughly estimated as $\sim s^3 n_\star = 3.7 \times 10^{-3}(\overline{m}/0.5\,\mathrm{M_\odot})^{3/2}$. Although this assumption is not negligible, the need of having two different canonical stars independently exerting their gravitational pull onto $\mathrm{PSR-B}$ and $\mathrm{PSR-E}$, makes the joint probability of such configuration suspiciously low, $\lesssim 10^{-5}$.

[1] If confirmed, such anisotropies would support the hypothesis of a relatively massive, probably binary black hole

Rather than being randomly placed, could the perturber be a binary companion to the MSPs? For such a companion not to have been already discovered by pulsar timing analysis would require an orbital period $P_b \gtrsim 20\,\mathrm{yr}$. Survival of such a wide binary is quite problematic in the core of a dense cluster like NGC 6752 — indeed no binary pulsar with $P_b > 3.8\,\mathrm{days}$ has been detected in collapsed clusters to date. Seeing two such systems in NGC 6752 appears extremely unlikely.

One may wonder if a *single* object, significantly more massive than a typical star in the cluster, could simultaneously produce the accelerations detected both in PSR-B and PSR-E. Recently, Colpi Possenti & Gualandris (2002) suggested the presence of a binary black-hole (BH) of moderate mass ($M_{\mathrm{bh+bh}} \sim 100 \div 200\,\mathrm{M}_\odot$) in the center of NGC 6752 in order to explain the unprecedented position of PSR-A, the binary millisecond pulsar which is $6'.4$ far away from the cluster center (D'Amico et al., 2002). As deduced from Figure 3.3, the projected separation of PSR-B and PSR-E is only $d_\perp = 0.03\,\mathrm{pc}$. A binary BH of total mass $M_{\mathrm{bh+bh}}$, approximately located in front of them within a distance of the same order of $d_\perp$, could be accelerating both the pulsars without leaving any observable signature on the photometric profile of the cluster. As the BH binarity ensures a large cross section to interaction with other stars, the recoil velocity v_{rec} due a recent dynamical encounter could explain the offset position (with respect to C_{grav}) of the BH. However this scenario suffers of a probability at least as low as that of the previous two: placing the black hole at random within the core gives roughly a 1% chance that it would land in a location where it would produce the observed pulsar accelerations and the required $v_{\mathrm{rec}} \gtrsim 4 \sim 5\,\mathrm{km\,s^{-1}}$ is also at the upper end of the expected distribution of v_{rec} for an intermediate mass black-hole in NGC 6752 (Colpi Mapelli & Possenti, 2003a).

In summary, on the basis of the available data, the accelerations shown by PSR-B and PSR-E can be easily accounted by the usually adopted hypothesis *(i)* (which could explain also the large positive $\dot{P}$ of PSR-D if it were not intrinsic), although the nature of the required extra amount ($1500 \div 2000\,\mathrm{M}_\odot$) of low luminosity mass still remains puzzling. The existence of local perturbator(s) of the pulsar dynamics (case *(ii)*) is a

distinct possibility. While it seems extremely unlikely purely on the basis of the high value of $\dot{P}/P$ measured in PSR-B and PSR-E, there are other indications of a binary low-mass BH. In particular, it would explain: *(a)* the absence of any cusp in the radial density profile, *(b)* the flat velocity dispersion profile (Xie et al., 2002), *(c)* and *(d)* the ejection of PSR-A and PSR-C in the cluster outskirts (Colpi Possenti & Gualandris, 2002). However it is admittedly an *ad hoc* hypothesis, requiring a fine tuned scenario.

Clearly additional information must be collected. A longer baseline for timing measurements will allow to better constrain the presence of companions in very large orbits around PSR-B and PSR-E. In particular it will permit to derive (at least) upper limits on the second derivative of the spin period of the pulsars, which is more influenced by by-passing stars rather than by the cluster potential well (Phinney, 1992). Similarly, the (single massive or binary intermediate mass) black-hole hypotheses could be better investigated with spectroscopic determination of the dispersion velocity of the stars located in the pulsars' neighborhood, likewise with star density counts reaching higher magnitudes (hence exploiting a larger sample of objects) and better spatial resolution (thus probing the innermost $1"$ of the cluster and the surroundings of the pulsars).

3.4 The Helium White Dwarf orbiting the Millisecond Pulsar in the halo of the Globular Cluster NGC 6752

As mentioned in the introduction to this chapter PSR J1911−5958A is the only binary millisecond pulsar associated to this cluster. It has a spin period of 3.26 ms, an orbital period of 0.84 days and very low eccentricity ($e < 10^{-5}$). Precise celestial coordinates ($RA = 19^{\rm h}11^{\rm m}42\overset{\rm s}{.}756$, DEC=$-59°58'26\overset{''}{.}91$) have been obtained for this source from pulsar timing observations (D'Amico et al., 2002) and recently refined (Corongiu et al., 2006). This position is far away ($\sim 6'.4$, corresponding to about 74 core radii), from the cluster optical center: indeed PSR J1911−5958A is the more off-centered pulsar among the sample of ~ 100 MSPs whose position in the respective cluster is known, and it suggests that this object might be the result of strong interactions occurred in the cluster core.

Since dynamical friction should have driven the binary towards the GC center in a timescale much shorter than the age of the cluster, the location of PSR J1911−5958A has been interpreted as a evidence for a strong dynamical interaction which occurred $\lesssim 1$ Gyr ago in the cluster core. Colpi Possenti & Gualandris (2002) explored a number of possibilities for the peculiar location of PSR J1911−5958A: a careful analysis led to discard the hypothesis of a primordial binary (born either in the halo or in the core of the cluster) and to reject also the possibility of a 3-body scattering or exchange event off core stars. Hence they conjectured that a more massive target (either a binary or a single intermediate-mass black hole, see also Colpi Mapelli & Possenti, 2003a; Colpi et al., 2003b) could have provided the necessary thrust to propel PSR J1911−5958A into its current halo orbit at an acceptable event rate.

As a part of large program devoted to the optical identification of MSPs companion in GCs, Ferraro et al. (2001) present the identification of the optical counterpart to the PSR J1911−5958A companion.

3.4.1 The Optical Companion of PSR J1911-5958A

Figure 3.4 shows the $U, U-V$ and $B, B-V$ CMDs for the stars (*large filled circles*) identified in the $80" \times 80"$ FORS1 sub-image centered at the nominal position of PSR J1911-5958A. Most of the stars trace a clean and well defined main sequence (MS) spanning almost 8 mags in the U band reaching $U \sim 26$. Only a few sparse objects, showing a blue excess, are visible on the left side of the MS. The most extreme blue objects in the CMDs are CO-WDs: once the MS is matched, they nicely overlaps the position of a CO-WDs population (shown as *small empty circles* in Fig. 3.4) observed in this cluster by Renzini et al. (1996) and Ferraro et al. (1997a). In particular, the colors and the luminosities of the three CO-WDs found here and of the previously observed population agree with the theoretical cooling sequence for $0.5 M_{\odot}$ hydrogen rich WDs (Wood, 1995) (drawn as *heavy dashed line* in Fig. 3.4).

On the basis of the accurate astrometric positions obtained from the photometric catalog, we identified a blue object (hereafter COM J1911−5958A) lying at only $0\farcs1$ from the nominal position of the MSP. The finding chart (in the B-band filter) for

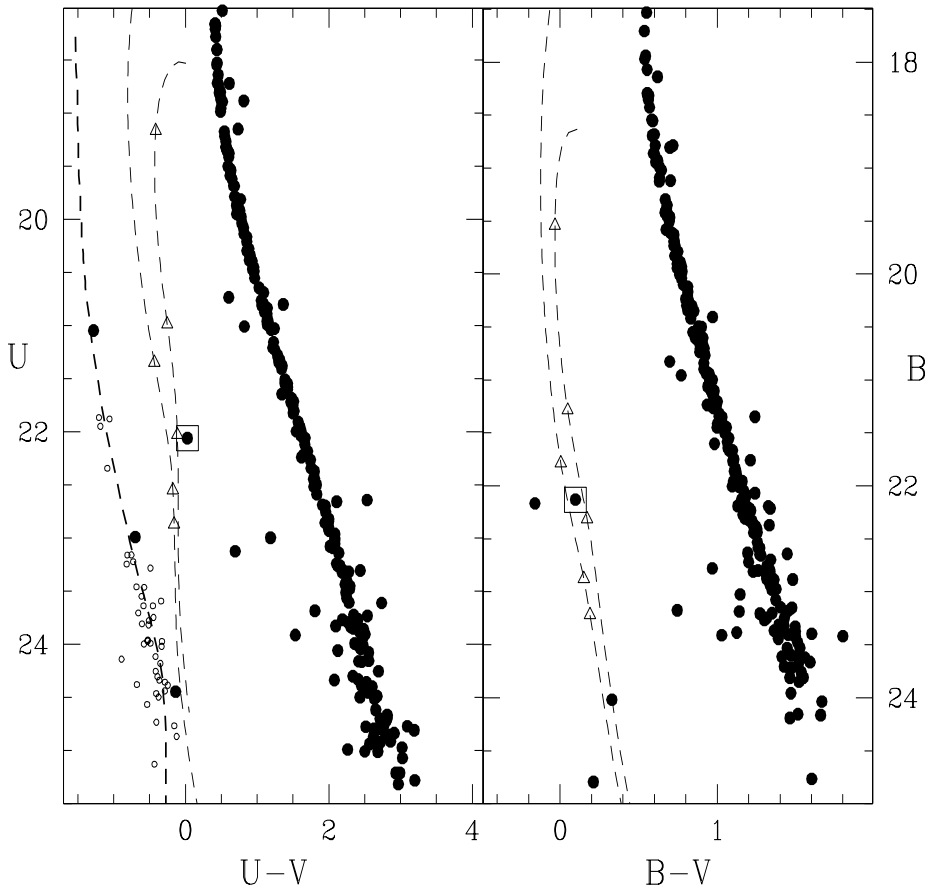

Figure 3.4: $((U, U-V))$ and $((B, B-V))$ CMDs for the stars identified in a region of 80×80 centered at the nominal position of the PSR J1911−5958A. The optical counterpart to the pulsar companion (COM J1911−5958A) is marked with a *large empty square*. The *heavy dashed line* is the CO-WD cooling sequence from Wood (1995); the two *light dashed lines* are the cooling tracks for He WD masses 0.197 and $0.172\,\mathrm{M}_{\odot}$ (the lowest mass model is the reddest one) from Serenelli et al. (2002). The *small triangles* along the two tracks label different ages (1, 2 and 3 Gyr, respectively). The CO-WD population observed in this cluster by Renzini et al. (1996) and Ferraro et al. (1997a) is also plotted as *small open circles* in the left panel.

COM J1911−5958A is shown in Figure 3.5. Only a few objects (~ 10) are lying in the region of the CMD to the left of the MS: considering the FoV of the sub-image, there

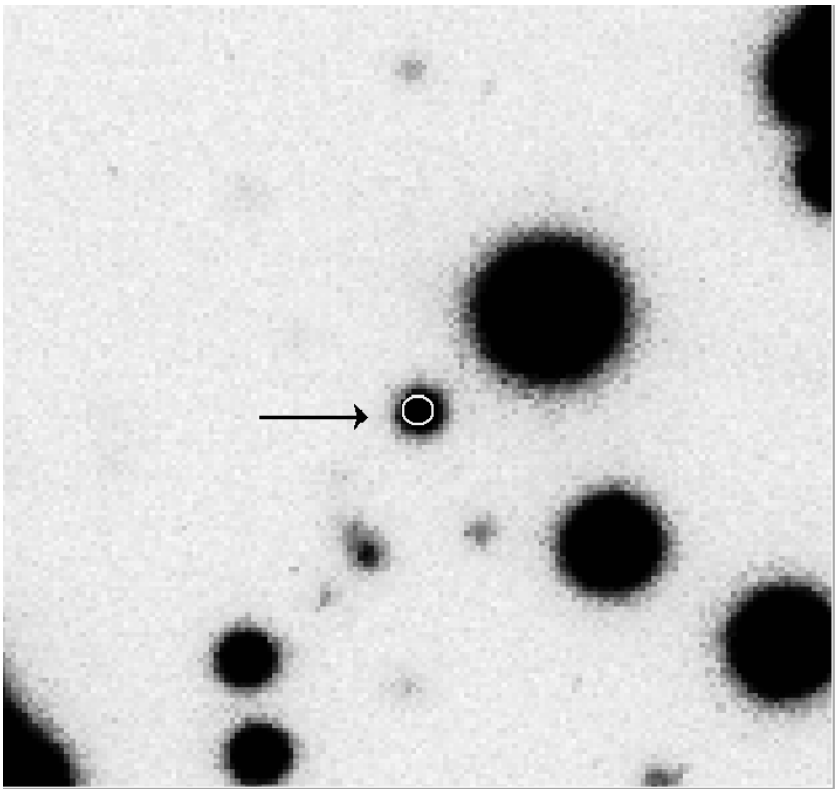

Figure 3.5: Finding chart for COM J1911−5958A showing the median-combined B-band image. The region covers 15×15, also plotted is the 1σ error circle ($0\farcs3$) for the absolute astrometric positioning of the optical image. North is up and East is to the left.

is a very small probability ($\lesssim 5 \times 10^{-3}$) of detecting one of the blue objects just by chance in a circular aperture of radius $\sim 0\farcs3$ (corresponding to the uncertainty in the relative radio-optical astrometry) centered on the pulsar position.

The position of COM J1911−5958A is marked as a *large empty square* in the CMDs in Figure 3.4, whereas absolute coordinates and magnitudes are listed in Table 3.1. Taking into account the expected variability of this object and the global uncertainty in the calibration of the photometric zero-point, the conservatively adopted overall uncertainty in the reported magnitudes is 0.15 mag.

The location of COM J1911−5958A in the CMDs (~ 1.5 mag bluer than the MS in the diagram) excludes that this star is a CO-WD, while it resembles U_{opt}, the companion to PSR J0024–7203U in 47 Tuc (Edmonds et al., 2001), which was suggested (Edmonds et al., 2001) to be a low mass Helium core WD (He-WD) from the comparison

with theoretical models by Serenelli et al. (2001). However, the He-WD tracks used by Edmonds et al. (2001) were computed for progenitors with high (solar) metallicity ($Z = 0.02$).

Here we have applied the same procedure taking advantage of a new set of tracks specifically computed (Serenelli et al., 2002) for globular cluster applications, i.e. assuming progenitors with low metallicities. In particular, the used cooling tracks have $Z = 0.001,$ which are closer to the cluster metallicity ($[Fe/H] = -1.43 \pm 0.04$) as recently derived by Gratton et al. (2003). The cooling sequences for two He-WD masses (0.172 and 0.197 $M_{\odot}$, respectively) are over-plotted in Figure 3.4 (*light dashed lines*). The models have been drawn by adopting a distance modulus $(m - M)_0 = 13.13$ (from the homogeneous distance scale for 61 GCs derived by Ferraro et al., 1999b) and a reddening $E(B - V) = 0.04$ (Harris, 1996; Gratton et al., 2003). Note that the distance modulus adopted here is consistent both with the estimate obtained from the WD cooling sequence ($(m-M)_0 = 13.05 \pm 0.1$) by Renzini et al. (1996) and with the most recent determination ($(m - M)_0 = 13.12 \pm 0.08$) derived from MS fitting by Gratton et al. (2003).

Inspection of Figure 3.4 reveals that luminosity and color of COM J1911−5958A well agree with its being a He-WD of mass in the range $0.17 - 0.20\,M_{\odot}$. In particular, from the $Z = 0.001$ models of masses $0.172\,M_{\odot}$ and $0.197\,M_{\odot}$ by Serenelli et al. (2002), we derive the following estimates for the properties of COM J1911−5958A: a temperature in the interval $T_{\rm eff} = 10,000 \div 12,000$ K, a gravity $\log g = 6.12 \div 6.38$, a luminosity $L = 0.03 \div 0.04\,L_{\odot}$, a radius $R = 3 \div 4 \times 10^9$ cm and a cooling age in the range $1.2 \div 2.8$ Gyr.

V	B	U	$\alpha_{\rm J2000}$	$\delta_{\rm J2000}$
22.03	22.13	22.06	$19^{\rm h}11^{\rm m}42\overset{\rm s}{.}743$	$-59°58'26\overset{''}{.}85$
$T_{\rm eff}$ (k)	gravity (log g)	luminosity $L_{\odot}$	radius cm	cooling age Gyr
$10,000 \div 12,000$	$6.12 \div 6.38$	$0.03 \div 0.04$	$3 \div 4 \times 10^9$	$1.2 \div 2.8$

Table 3.1: Photometric data, position & characteristics inferred for COM J1911−5958A.

From the pulsar mass-function ($0.0026887\,M_{\odot}$, D'Amico et al., 2002), it results a

minimum companion mass (corresponding to a system seen edge-on, i.e. with orbital inclination $i = 90°$) $M_{\rm COM} = 0.185\,{\rm M}_\odot$ for a pulsar mass of $1.35\,{\rm M}_\odot$ (Thorsett & Chakrabarty, 1999). Given the upper limit ($M_{\rm COM} \lesssim 0.2\,{\rm M}_\odot$) of the range of masses of COM J1911−5958A inferred from the cooling tracks of Serenelli et al. (2002), we can constrain the inclination i to be larger than $\gtrsim 70°$. Adopting a larger value for the pulsar mass would result in a even larger lower limit for the orbital plane inclination.

Dynamical friction can rapidly drive back to the cluster core an object of total mass of order 1.6 $\rm M_\odot$ moving on a highly eccentric orbit in the cluster potential. In particular, ejection of PSR J1911−5958A from the core to the outskirts of NGC 6752 (implying a radial orbit) cannot be occurred more than $\tau_{\rm df} = 0.7 \div 1$ Gyr ago (Colpi Possenti & Gualandris, 2002). The cooling age of COM J1911−5958A is longer than $\tau_{\rm df}$, implying that any dynamical event responsible for the ejection probably acted on an already recycled millisecond pulsar. Hence, the optical identification of COM J1911−5958A tends to exclude *(i)* the scenarios in which the recycling process occurred after (or was triggered by) the dynamical encounter which propelled the pulsar in the cluster halo (but see the discussion in Sigurdsson, 2003) and *(ii)* any kinds of interactions imparting a significant eccentricity to the binary pulsar (having excluded a recent mass transfer phase, the circularization of the system at the present level, $e \simeq 10^{-5}$, would require a time much longer than $\tau_{\rm df}$). In particular, among the proposed black hole hypotheses (Colpi Mapelli & Possenti, 2003a; Colpi et al., 2003b) a binary black hole of mass in the range $10 \div 200\,{\rm M}_\odot$ seems the most plausible candidate.

Stimulated by the implications of the peculiar position of PSR J1911−5958A in NGC 6752, we have undertaken a program of optical observations, in the aim of shedding light on the origin and evolution of the binary and for assessing its belonging to the cluster. As a first step, we have identified the radio pulsar's optical companion (hereafter COM J1911−5958A, an analogous identification was independently achieved by Bassa et al. 2003) by using high-resolution images taken at ESO Very Large Telescope: in the following sections we present the results of a second group of photometric and spectroscopic observations performed at ESO Very Large Telescope (VLT) in order to determine the radial velocity (§5) and light curve (§7) of COM J1911−5958A. The mass

ratio of the system is derived in §6, as well as contraints on the pulsar mass and the orbital inclination of the binary.

3.5 Radial velocity curve of COM J1911−5958A

The analyzed spectra has been retrieved from the ESO Science Archive Facility. Observations were performed by using the *FOcal Reducer and low resolution Spectrographer 1* (FORS1) mounted at the *Antu* 8m-telescope (UT1) of the ESO-VLT on Cerro Paranal (Chile). The spectra series were obtained during 6 different nights from 2004 July to 2004 August, using the Long Slit Spectroscopy (LSS) operation mode and the B-Bessel Grism, which cover the spectral range $3400 - 5900$Å. The $1'$ wide and $6'.8$ long slit was adopted, yelding a dispersion of 1.2 Å/pixel. The exposure time for each spectrum (2500 sec, $\sim 4\%$ of the system orbital period), and the total number of different spectra analyzed (23), ensured a typical signal-to-noise ratio $S/N \simeq 10$ per pixel (measured at the continuum level), allowing to collect a good phase-resolved set of data. The data reduction has been perfomed by using the standard IRAF[2] tools. Raw images has been first corrected for bias and flat-field and decontaminated from cosmic rays, then the spectra were extracted and wavelenght calibrated. Using the task IDENTIFY and polynomial fit with a 4-th order function, the accuracy of the wavelenght calibration results ≤ 0.01 Å. Each spectrum has been corrected for the Earth motion and reported to a common heliocentric system using the task RVCORRECT.

A median combined spectra is shown in Fig 3.6

The spectral range covered by the spectra allows the observation of several spectral features, in particular the Hydrogen Balmer-lines from H_β to $H(7)$. The Doppler-shifted wavelenght of each line has been measured by using the SPLOT task, fitting with a gaussian function all the features. The wavelenght of each line has been converted to a radial velocity (RV), then all the RVs measured for each spectra has been averaged and a mean value was obtained (accounting for the heliocentric correction). Only the 21

[2]IRAF is distribuited by the National Optical Observatory which is operated by the Association of Universities for Research in Astronomy Inc., under cooperative agreement with the National science Foundation

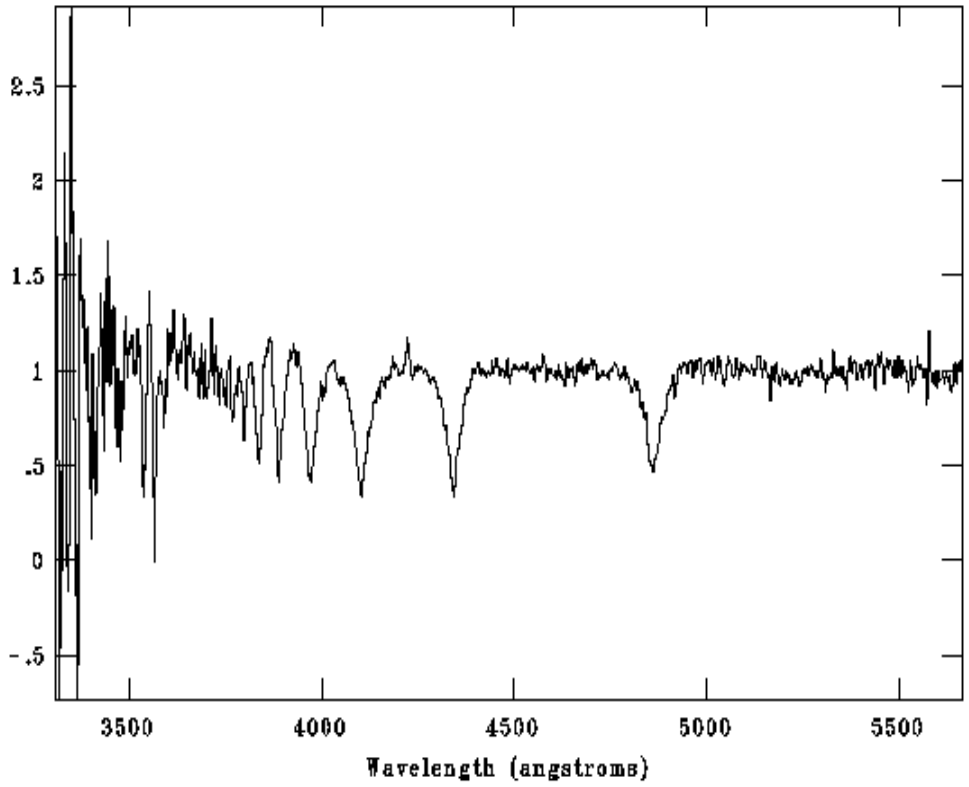

Figure 3.6: Median combined spectra obteined from the 23 singular exposures analyzed: the continuum is normalized to the units and the Hydrogen Balmer-lines from H_β to $H(7)$. are cleary visibles.

RV determinations resulting from the average of at least five measures have been used. The mid-point of each observations has been converted to a orbital phase by adopting the orbital period and the epoch of the ascending node for the pulsar orbit as given by the radio ephemeris (Corongiu et al., 2006). Phases 0.0 and 0.5 correspond to the quadratures, phase 0.25 to the inferior conjunction of the companion (i.e. when COM J1911−5958A is at its closest position with respect to the observer) and phase 0.75 to the superior conjunction. In order to determine the amplitude K of the radial velocity curve and the systemic velocity γ of the binary system, we have fitted the data by using a function which is the sum of a constant and a sinusoid, adequate to describe the almost perfectly circular orbit of COM J1911−5958A. The best fit curve yields $K = 237.5 \pm 20.0$ km s^{-1}

and $\gamma = -28.1 \pm 4.9$ (1σ uncerteinties) and is reported in Figure 3.7.

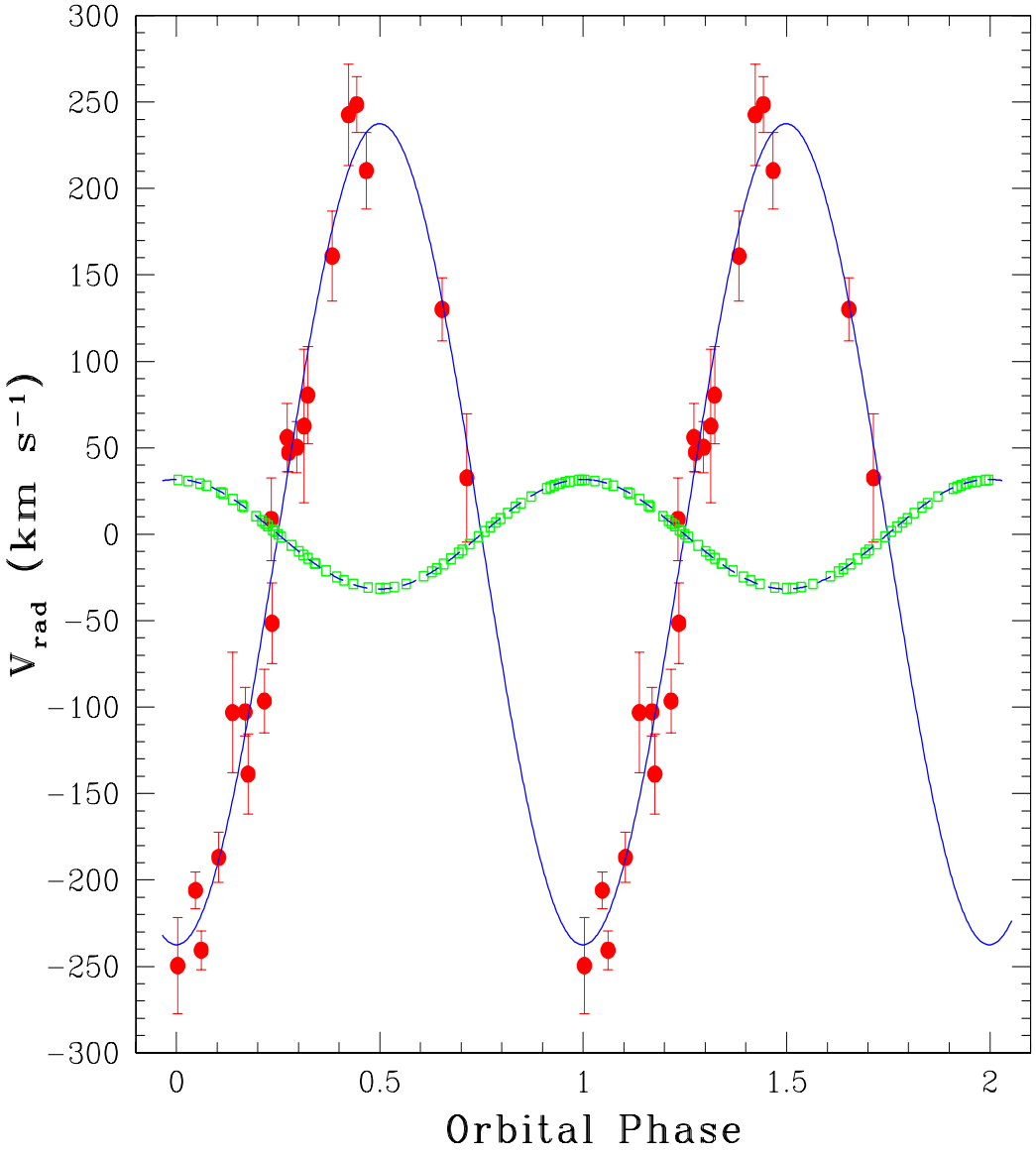

Figure 3.7: Velocity curves of COM J1911−5958A (*large dots*) and PSR J1911−5958A (*empty squares*). The data for the pulsar are derived from timing measurements and the radio ephemeris (Corongiu et al. 2006). Error bars for the pulsar radial velocity are smaller than the size of the symbols. The *dashed* and the *solid lines* represent the best-fit to the velocity data with a sinusoidal curve, for the pulsar and the companion star, respectively. The systemic velocity $\gamma = -28.1$ km s^{-1} of the binary has been subtracted.

3.6 The mass ratio

The systemic velocity of the binary system is in agreement with the published radial motion of the globular cluster ($v_{\rm NGC6752} = -27.9 \pm 0.8$, Harris et al. 1996, catalog revision 2003). This lends further support to the cluster membership of the binary. Given the central 1-D dispersion velocity of NGC 6752 (9-15 km s^{-1}, Drukier et al. 2003), the expected 1-D dispersion velocity for objects of mass $1.4 - 1.7$ M$_\odot$ (corresponding to the most likely total mass of the binary, see later) and located at the projected position of PSR J1911−5958A with respect to the cluster center is 2-3 km s^{-1} (Mapelli, private communication). This is fully compatible with the value of the difference $\Delta v_{\rm 1D} = |\gamma - v_{\rm NGC6752}| \lesssim 6$ km s^{-1}. Moreover, the small value of $\Delta v_{\rm 1D}$ may indicate that the binary is now near apoastron of a highly elliptical orbit in the potential well of the globular cluster. In fact, were the binary on an almost circular orbit at 74 core radii from the GC center, its line of sight velocity with respect to the cluster center (Sabbi et al. 2004), as estimated from the enclosed mass, would be of the order $\gtrsim 12$ km s^{-1}. All these considerations support the hypothesis that the binary has been recently kicked out of the core of NGC 6752 due to a dynamical interaction (see §4).

We are in the position of inferring the ratio between the masses of the two stars in the binary. The mass function of the pulsar, as measured from radio observation, is (Corongiu et al. 2006,):

$$f(M_{PSR}) = \frac{M_{\rm COM}^3 \sin^3 i}{(M_{\rm COM} + M_{\rm PSR})^2} = 0.002687849(6)\ {\rm M}_\odot, \tag{3.1}$$

whereas the mass function of the companion, derived from our spectroscopic observation results:

$$f(M_{\rm COM}) = \frac{M_{\rm PSR}^3 \sin^3 i}{(M_{\rm COM} + M_{\rm PSR})^2} = \frac{K^3 P_{\rm orb}}{2\pi G} = 1.13 \pm 0.29\ {\rm M}_\odot, \tag{3.2}$$

where $P_{\rm orb} = 0.83711347700(1)$ days (Corongiu et al. 2006), K is the amplitude of the radial velocity curve, $M_{\rm PSR}$ and $M_{\rm COM}$ are the masses of the pulsar and the companion, i is the inclination of the normal to the orbital plane with respect to the line-of-sight, and the brakets report the 1σ errors on the last significant digit. The mass ratio $q = M_{\rm PSR}/M_{\rm COM}$ can be derived by combining eq. (3.1) with eq. (3.2), and results $q = 7.49 \pm 0.64$.

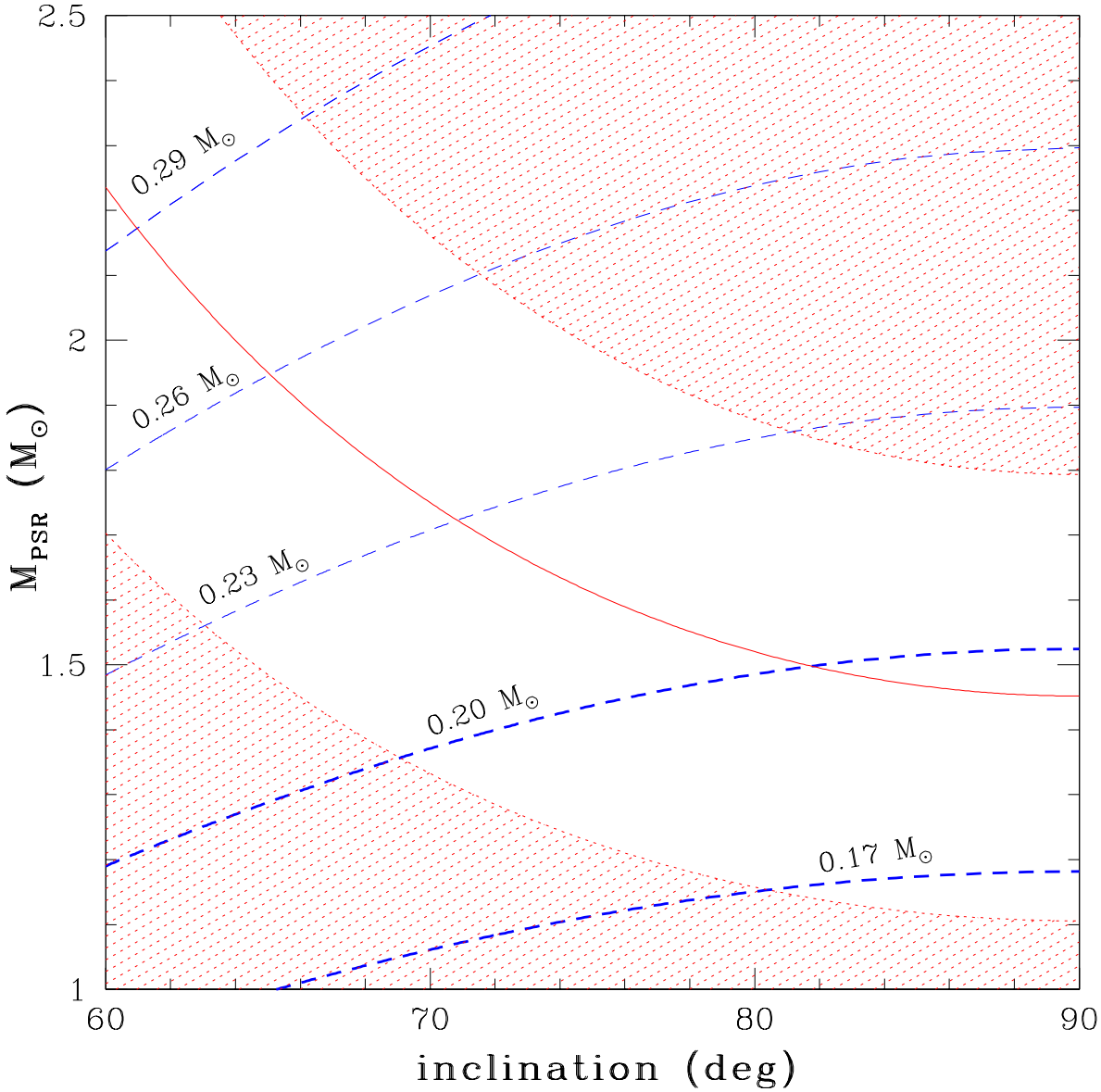

Figure 3.8: Mass of PSR J1911−5958A and orbital inclination of the binary. The allowed range of values are constrained to lie within the strip whose borders (*dotted lines*) are the 1σ boundaries derived from the mass ratio of the system. Lines of constant mass for COM J1911−5958A are also shown (*dashed lines*) and labeled with the assumed mass value. If COM J1911−5958A is a He-WD, the space of parameters is additionally constrained (see Ferraro et al. 2003a) between the lines corresponding to companion masses 0.17 and 0.20 $M_\odot$ (*thick dashed lines*).

Solving separately for the masses of the two stars would require a determination of the orbital inclination: the relation between $M_{\rm PSR}$ and i for different values of $M_{\rm COM}$ is

displayed in Figure 3.8, for a reasonable choice of the neutron star mass ($1 - 2.5$ $\mathrm{M}_{\odot}$, Shapiro & Teukolsky 1983). The measured mass ratio (with its uncertainty) selects a narrow strip of allowed parameters in Figure 3.8. In particular, $M_{\mathrm{PSR}} > 1.1$ $\mathrm{M}_{\odot}$ and $M_{\mathrm{COM}} > 0.16$ $\mathrm{M}_{\odot}$ (1σ limits). Moreover, $M_{\mathrm{COM}} \lesssim 0.30$ $\mathrm{M}_{\odot}$ and the orbital inclination is $\gtrsim 60^{\circ}$. Tighter constraints can be obtained in the hypothesis that the companion is a He-WD: in this case, the range of masses determined by Ferraro et al. (2003a) implies that the system is almost edge-on ($i \gtrsim 70^{\circ}$) and the pulsar mass is in the range $1.2 - 1.5$ $\mathrm{M}_{\odot}$. It is worthwhile to note that the latter mass interval brackets the values of all neutron star masses accurately measured so far (Lorimer 2005), but one case (Nice et al. 2005).

3.7 The puzzling light curve of COM J1911−5958A

The photometric observations were performed in service mode at the *Antu* 8m-telescope of the ESO-VLT during two nights in 2003, March and May (ESO Program ID 071.D-0232), and six nights in 2004, August (ESO Program ID 073.D-0067A). All the images were acquired using B-band filter in high-resolution mode with the FORS1 camera. In this configuration the instrumental pixels scale is $0.1\ ''pixels^{-1}$ and the Field of View of the 2048×2048 pixels Tektronix-CCD is $3'.4 \times 3'.4$. The data comprise twenty-one 600s and five 360s exposures, centered roughly less then $1'$ far from the PSR J1911−5958A nominal position (D'Amico et al. 2002). The observations on 2004 were planned in order to be randomly distributes along the orbit of the binary system.

From all the original frames we have extracted a subimage of 500×500 pixels, roughly centered on the nominal position of PSR J1911−5958A. The scientific images have been reduced using ROMAFOT, a package specifically developed to achieve accurate photometry in crowded fields (Buonanno et al. 1983); it enables the visual inspection of the quality of point-spread function (PSF) procedure. PSF best-fitting has been performed for all the images separately, and the mask with the star position obtained from the best-quality image was adapted to each image. The instrumental magnitudes have been reported to a common photometric system, then we have obtained a catalog with the coordinates and the instrumental magnitudes for all the stars common to all the images.

We have performed the photometric calibration using two different and indipendent methods. First, magnitudes have been matched to four standard stars (Landolt 1992) observed under photometric conditions in the B-band. Then, all the ~ 100 stars in our catalog in common with the B-band catalog published by Ferraro et al. (2003) have been used to derive the photometric zero-point. The two resulting calibrations are fully consistent within a few hundredths of magnitude.

A periodicity search was carried out on the photometric data set using GRATIS (GRaphycal Analyzer of TIme Series), a software package developed at the Bologna Astronomical Observatory (see previous applications in Ferraro et al. 2001). Since the period ($P = 0.839 \pm 0.002$ day) obtained from the COM J1911$-$5958A variability curve turned out to be fully consistent with that obtained from the radio time series of PSR J1911$-$5958A, a phased light curve has been produced (Figure 3.9) assuming the same orbital parameters used in §5. The different symbols in Figure 3.9 mark series of B-magnitudes obtained in different observing nights (hence different companion's orbits): in particular, empty and starred symbols are used for the pointings of 2004, whereas filled symbols (clustering at about phase 0.6) refer to observations of 2003.

The result is really surprising: COM J1911$-$5958A shows two phases of strong enhancement of the luminosity located close to the quadratures and extending for about 20% of the orbit each. The primary maximum occurs between phases 0.5 and 0.6 (a more precise positioning is prevented by the lacking of useful data in that range) with a flux variation of $\gtrsim 0.3$ mag in less than 1 hr: orbital location and rapidity of the brightening are confirmed in two different orbits. A secondary maximum, corresponding to a brightening of ~ 0.2 mag appears at about phase 0.05, presenting a less steep raise with respect to the primary peak (in this case only the decay from the maximum is observed in two different orbits). Outside the peaks, the source displays an almost steady luminosity at an average $B = 22.11 \pm 0.02$. In particular the B-band luminosity at orbital phase ~ 0.6 does not show any significant fluctuation between the 2003 and the 2004 data (the pointings of 2003 unfortunately did not cover other orbital phases).

These features are unusual and intriguing. The modulation of the optical light curve of the companion to a MSP is most often driven by the heating of one emisphere of the

star (whose rotation is syncronized with the orbital period) due to the radiation coming from the pulsar: see for example the cases of PSR B1957+20 (Callanan, van Paradijs, & Rengelink 1995) and PSR J2051-0827 (Stappers et al. 2001) in the Galactic field and 47 Tuc U and 47 Tuc W in the GC 47 Tucanae (Edmonds et al. 2001, 2002). For PSR J1911−5958A the square of the ratio ($\xi_1 \sim 100$) between the orbital separation ($\sim 4.5 - 5 \mathrm{R}_\odot$) and the radius of the companion (inferred from the off-peaks luminosity and the effective temperature, Ferraro et al. 2003a) is much larger than the ratio ($\xi_2 \sim 25$) between the rotational power of the pulsar[3] and the bolometric off-peaks luminosity of COM J1911−5958A. This implies that the modulation due to the heating effect ($\Delta(\mathrm{mag}) = 2.5 \log[1+(\eta/2)(\xi_2/\xi_1^2)]$, where $\eta < 1$ is the efficiency of the process) should be negligible ($\Delta(\mathrm{mag}) \lesssim 0.001$) and in fact no flux enhancement is detected around phase 0.75, when the side of the companion facing the pulsar is visible.

Ellipsoidal variations due to the tidal deformation of the companion are known to produce a light curve with two peaks at quadratures (see for example the case of PSR J1740−5340 in NGC 6397, Ferraro et al. 2001), but the light curve is expected to have maxima of equal amplitude and clear minima (of unequal depth) at conjunctions. Moreover, tidal deformations are expected to be insignificant for a companion whose radius is ~ 20 times smaller than the radius of its Roche lobe.

Accretion of matter onto a compact object can generate a variety of modulated optical emission (e.g. Frank, King & Raine 2002), but neither the neutron star nor the He-WD in this system can be suitable sources of plasma feeding accretion-related processes at the present epoch. The timing stability and the extension of the time span of the radio observations of PSR J1911−5958A tend also to exclude the existence of a residual accretion disk around the pulsar or the presence of a third optically faint body which is now pouring mass in the binary.

One may wonder if the optical modulation can be intrinsic to the He-WD. Non-radial

[3]It is calculated with the usual formula $\dot{L}_{\mathrm{rot}} = (4\pi^2) I \dot{P}/P^3$ where I (assumed equal to 10^{45} g cm^2) is the neutron star moment of inertia, P the spin period and $\dot{P}$ the spin period derivative. Given the observed proper motion and the off-centered position of PSR J1911−5958A in NGC 6752, the value of $\dot{L}_{\mathrm{rot}}$ can be underestimated at most a factor 3 as a consequence of the centrifual acceleration of the pulsar and of the combined effects of the gravitational potentials of the Galaxy and of the globular cluster (Corongiu et al. 2006). This possible correction leaves the discussion about the heating effect unchanged.

pulsations of WDs can produce optical fluctuations at a level of ~ 0.2 mag, but for a star with $T_{\rm eff} \approx 11,000\ K$ the expected modulation occurs at periods significantly shorter than 0.84 days (e.g. Bergeron et al. 2004). However, a few high magnetic field ($\sim 10^8$ G) isolated WDs (see e.g. PG 1031+234, Piirola & Reiz 1992, and EUVE J0317−855, Barstow et al. 1995) display variations of $\lesssim 0.3$ mag at the supposed rotational period of the star. In the framework of an oblique rotator model for the WD, these photometric modulations have been interpreted with changes with the rotational phase of the mean magnetic field strenght over the visible stellar surface (which in turn affects the opacity along the line of sight: Ferrario et al. 1997). A suitable geometry (leading to an alternate exposure of both the magnetic polar caps of the WD) may in principle produce a double peaked light curve, but we note that all the aforementioned effects have been observed only in relatively massive WDs ($\sim 0.5 - 1.0\ \rm M_{\odot}$) sofar.

Given this puzzling scenario, further data are clearly necessary for constraining the origin of the optical modulation in this system, namely phase resolved multi color (UBVRI) photometry, complemented with higher resolution spectroscopy.

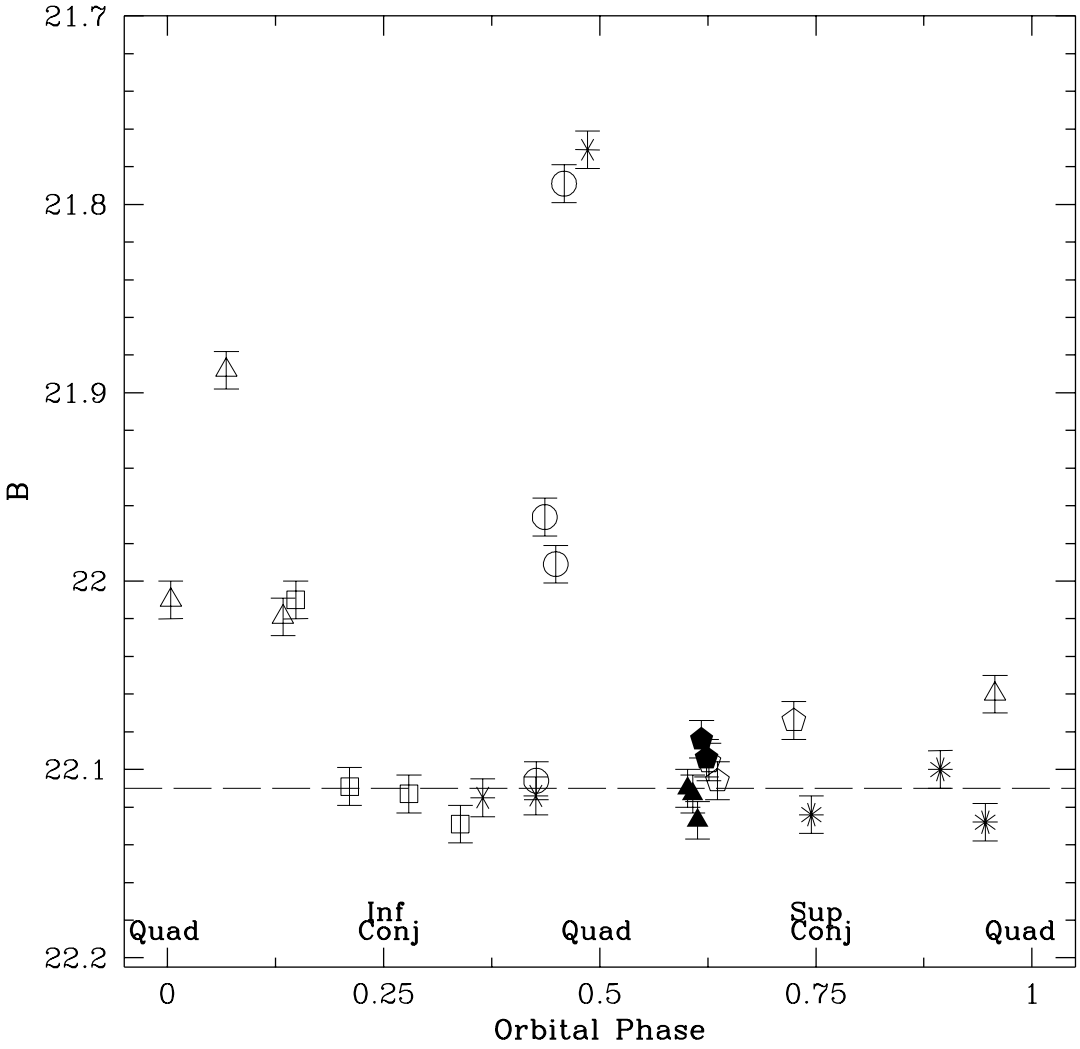

Figure 3.9: Light curve of COM J1911−5958A: the *filled* symbols represent observations performed on two different nights on March and May 2003, whereas the *empty* and *starred* symbols represent the data collected on August 2004. Different marks refer to different nights of observation. The horizontal *dashed line* represents the off-peaks mean B-magnitude of the source, calculated averaging the data at orbital phases in the ranges (0.2−0.4) and (0.6−0.95). The phases of quadrature and conjunction of COM J1911−5958A are reported for clarity.

Chapter 4

Discovery of a tidally deformed millisecond pulsar companion in NGC6266

4.1 Millisecond Pulsars in NGC6266

NGC 6266 (M62) is one of the most massive and brightest ($M_V = -9.19$; Harris 1996[1]) Galactic Globular Clusters (GCs), also characterized by high values of the central density (log $\rho_0 \sim 5.47$, with ρ_0 in units of $M_\odot$ pc^{-3}; Beccari et al. 2006) and reddening ($E(B-V) \sim 0.47$; Harris 1996). It displays a King-model density profile with an extended core ($\sim 19''$) and a modest value of the concentration parameter ($c = 1.5$, Beccari et al. 2006). Six binary millisecond pulsars (MSPs) have been discovered in M62 (D'Amico et al. 2001, Jacoby et al. 2002, Possenti et al. 2003, hereafter P03) and it ranks fifth of the GCs in wealth of MSPs, after Terzan 5, 47 Tucanae, M15 and M28[2]. Surprisingly, all MSPs in NGC 6266 are in binary systems. As discussed in P03, the absence of known isolated MSPs in NGC 6266 cannot simply be ascribed to a selection effect since, for a given spin period and flux density, an isolated MSP is easier to detect than a binary one. Thus if such a lack of isolated pulsars is not a statistical fluctuation, it must be somehow related to their formation mechanism and to the dynamical state of the cluster. Moreover, recent deep *Chandra* X-ray observations of NGC 6266 have revealed a

[1]When referencing to Harris (1996) we intend the updated dataset at `http://www.physics.mcmaster.ca/Globular.html`

[2]See `http://www.naic.edu/ pfreire/GCpsr.html` for an updated catalogue of MSPs in GCs with relatives references

very large number of X-ray sources: 51 sources were detected within the cluster 123 half mass radius (Pooley at al., 2003), indicating that an high number of cataclysmic (and/or interacting) binaries should be present.
These observational facts may suggest that NGC 6266 is in an "active" dynamical state, where the rate $\mathcal{R}_{\rm form}$ of formation (and hardening) of binary systems containing a neutron star and/or a white dwarf is much larger than the rate of disruption $\mathcal{R}_{\rm disr}$ of such systems (Pooley & Hut, 2006).

P03 presented phase–connected timing solutions, yielding precise celestial coordinates, for three of the MSPs in NGC 6266 (see Fig.4.1); all this pulsars are located close to the center of mass of the cluster, at least in projection, with projected distances $r \lesssim 2\ r_c$ where r_c is the core radius of NGC6266. The position of the three pulsars is consistent with the fact that dynamical friction and thermal equilibrium, in which energy equipartition gives less velocity to the most massive species, costraining them to reside deep in the potential well. The spin period derivatives, $\dot{P}$, are all negative, implyng that the line-of-sight acceleration imparted to the pulsars is directed towar the observer and it overcomes the (positive) intrinsic $\dot{P}_i$ due to the spin-down.

One of the three pulsars, PSR J1701−3006B (hereafter PSR 6266B) displays partial or total eclipses of the radio signal at 1.4 GHz near its superior conjunction (in the convection adopted throughout this paper, this corresponds to orbital phase $\phi = 0.25$), clearly due to gas streaming off the companion. The pulsar orbit is circular with a projected semi-major axis of only $R \sim 0.11\ \mathrm{R}_\odot$.

P03 suggested two options for explaining the behaviour of the PSR 6266B system: *(i)* the pulsar companion is a non-degenerate bloated star, whose mass loss is sustained by ablation of its loosely bound surface layers by the relativistic wind emitted by the pulsar. In this case, PSR 6266B may resemble PSRs B1957+20 (Fruchter et al. 1990) and J2051−0827 (Stappers et al. 2001): the optical light curve of their companion star presents a maximum when we see the side of the companion facing the pulsar (i.e. at the pulsar inferior conjunction: $\phi = 0.75$), a clear signature of the irradiation of the companion surface by the pulsar flux; *(ii)* the pulsar companion is a tidally deformed star overflowing its Roche lobe due to the internal nuclear evolution. In this case, the

Parameter	PSR J1701−3006A	PSR J1701−3006B	PSR J1701−3006C
	Observed Parameters		
R. A. (J2000.0)	17 01 12.5127 (3)	17 01 12.6704 (4)	17 01 12.8671 (4)
Decl. (J2000.0)	−30 06 30.13 (3)	−30 06 49.04 (4)	−30 06 59.44 (4)
Period, P (ms)	5.2415662378289(16)	3.5938522173305(14)	3.8064243637728(18)
Period derivative, $\dot{P}$	$-1.3196(9) \times 10^{-19}$	$-3.4978(7) \times 10^{-19}$	$-3.189(11) \times 10^{-20}$
Epoch (MJD)	52,050.0	52,050.0	52,050.0
DM (cm^{-3} pc)	115.03 (4)	113.44 (4)	114.56 (7)
Orbital period, P_b (days)	3.805948407 (16)	0.1445454304 (3)	0.2150000713 (15)
Projected semimajor axis, x (lt-s)	3.483724 (8)	0.252775 (13)	0.192880 (12)
Eccentricity[a], e	$<4 \times 10^{-6}$	$<7 \times 10^{-5}$	$<6 \times 10^{-5}$
Time of ascending node, T_{asc} (MJD)	52,048.5627980 (15)	52,047.2581994 (9)	52,049.855654 (2)
Span of timing data (MJD)	51,714–52,773	51,714–52,773	51,714–52,773
Number of TOAs	80	74	73
rms timing residual (μs)	21	26	32
Flux density at 1400 MHz, S_{1400} (mJy)	0.4 (1)	0.3 (1)	0.3 (1)
	Derived Parameters		
Galactic longitude, l (deg)	353.577	353.573	353.572
Galactic latitude, b (deg)	7.322	7.319	7.316
Mass function, f_p ($M_\odot$)	0.00313392 (2)	0.00082999 (13)	0.00016667 (3)
Companion mass, M_c ($M_\odot$)	>0.20	>0.12	>0.07
Radio luminosity, L_{1400} (mJy kpc^2)	19 (7)	14 (6)	14 (6)
Offset, $\Theta_\perp$ (arcsec)	19.2	1.7	10.5

Figure 4.1: All the observed and derived parameters for three Pulsars in the globular cluster NGC6266

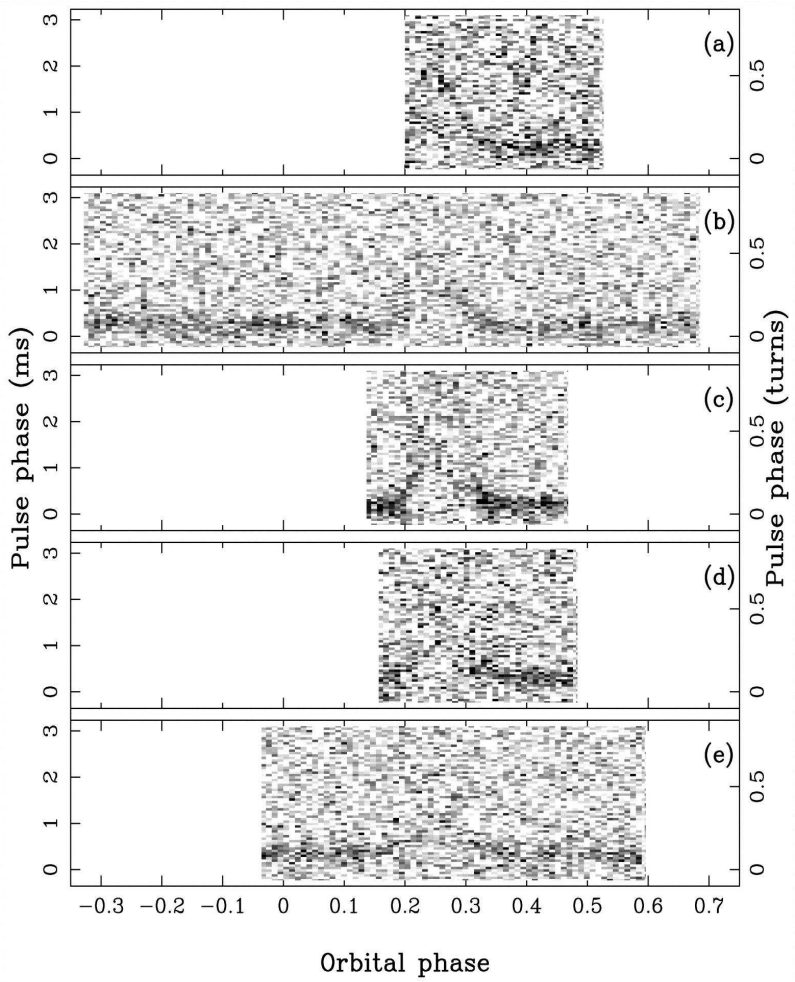

Figure 4.2: Eclipse of the radio signal at 1390 Mhz; the eclypses occurs at orbital phase ~ 0.25 (at the superior conjunction). A typical event starts at phase 0.15-0.20 and ends at phase ~ 0.35. In the five boxes are shown different kind of eclipses during five different observations

system may be more alike PSR J1740−5340 (D'Amico et al. 2001; Ferraro et al. 2001), where irradiation effects are negligible (Orosz & van Kerkwijk 2003) and the optical light curve of the companion is dominated by ellipsoidal variations (Ferraro et al. 2001), i.e. it shows two maxima at quadratures ($\phi = 0.0$ and 0.5). We here present the identification of the optical companion to PSR 6266B based on high-quality phase-resolved photometry obtained with the *Hubble Space Telescope* (HST) and X-ray emission detected with *Chandra* .

4.2 Observations and data analysis

4.2.1 *HST observations.*

The photometric data presented here consist of a set of high-resolution images obtained on 2004 August 1 by using the Advanced Camera for Survey (ACS), on-board the HST, and retrieved from the *ESO/ST-ECF Science Archive*. The data comprise three R-band exposures ($2 \times 340\,s$ and $1 \times 30\,s$ exposures), two (of 120 and 340 s each) B-band exposures and four (of 340, 1050, 1125, 1095 s each) H_α-band exposures. The three longest exposures in H_α are the combination of three sub-exposures. An additional set of Wide Field Planetary Camera 2 (WFPC2, Prop. 10845, PI:Ferraro) data has been secured through the H_α filter with the specific aim of testing the possible variability of the companion: ten[3] 1200 s exposures have been performed between May 2 and May 5 2007. In order to best resolve stars in the most crowded regions, the WFPC2 observations were performed by pointing the Planetary Camera (with a resolution of $0.046\ ''$/pixel) on the cluster center. The photometric analysis of the ACS dataset has been carried out using the ACS module of the Dolphot[4] package (Dolphin, 2002), using the FLT.fits datasets for the photometry, and the drizzled images as references for the geometric distortion correction. We have set the photometry parameters as recommended in the Dolphot manual, obtaining a final catalog of B, R and H_α magnitudes, calibrated according to Sirianni et al. (2005). The final catalog has been reported to an absolute astrometric system by cross-correlating the stars in common with the data set of Beccari et al. (2006), which has been astrometrized by using the standard stars from the new *Guide Star Catalog II* ($GSCII$) lying in the considered field of view (FoV). At the end of the procedure, the rms residuals were of the order of $\sim 0".5$ both in RA and Dec; we assume this value as representative of the astrometric accuracy.

In order to carefully search for any variability from the MSP companion, we have reanalyzed the H_α images in a small area around the nominal position of PSR 6266B by

[3]Only nine exposures have been used in the following analisys since one of the ten was usefulless because of a cosmic ray passage.

[4]The DOLPHOT packages, including the ACS module and all the documentation, can be found at `http://purcell.as.arizona.edu/dolphot/`.

using ROMAFOT (Buonanno et al. 1983). This package has been specifically developed to perform accurate photometry in crowded fields, that also allows a visual inspection of the quality of the PSF-fitting procedure. In particular, we have extracted 50×50-pixels ($\sim 2".5 \times 2".5$) sub-images from the ten original H_α ACS frames, each centered on the nominal position of PSR 6266B. In order to optimize the detection of faint objects, we have performed the search procedure on the median image. Then, the resulting mask with the star positions has been adapted to the individual sub-images, and the PSF-fitting procedure performed separately on each of them. The same strategy has been adopted for the analysis of the nine WFPC2 H_α images, after the careful alignement with the previously astrometrized ACS frames. The resulting instrumental magnitudes have been transformed to a common system, and a final catalog with coordinates and magnitudes for all the stars identified in the considered 19 sub-images has been compiled. The photometric calibration of the instrumental magnitudes and the absolute celestial coordinates were determined by using all the stars in common with the overall ACS catalog, calibrated and astrometrized as discussed above.

4.2.2 *Chandra Observations.*

NGC 6266 was observed for 63 ks on May 2002 with the *Chandra* Advanced CCD Imaging Spectrometer (ACIS). The ACIS-S3 chip was pointed on the cluster center, its field of view ($8' \times 8'$) entirely covering the half-mass radius ($1'.23$, Harris 1996). The data were reduced using the CIAO software (v. 3.3.0), reprocessing the level 1 event files; the task `acis_run_hotpix` was used to generate a new badpixel file. Then we applied the corrections for pixels randomization, good time intervals and grades. Our analysis includes only photons with ASCA grades of 0, 2, 3, 4 and 6. About 1.5 ks of observations were not considered in the analysis because of the high background level. We searched for discrete sources in our level 2 event file using `Wavdetect` (Freeman et al. 2002), performing the source detection separetely on the 0.2-1, 1-2, 2-8, and 0.2-8 keV bands. The detection treshold was set to 10^{-5}, and the source detection was performed increasing the sequence of wavelets from 1 to 16 by factors of $\sqrt{2}$. More than 110 sources were detected in the 0.2-8 keV band in the entire chip. The astrometry of all the detected

sources was corrected by using the Aspect Calculator provided by the *Chandra* X-Ray Center. Then we searched for possible optical counterparts both in our HST images and catalog. About 5 bright stars and 2 faint and extended objects (likely background galaxies) were found to coincide with the X-ray sources well outside the half-mass radius, where the stellar density is relatively low. We therefore used these optical counterparts for extending the astrometric solution of HST to the *Chandra* sources, thus obtaining the same accuracy in the absolute astrometry for both the optical and the X-ray sources.

4.3 Results

Fig. 4.4 shows the $3" \times 3"$ H_α WFPC2 map centered on the PSR 6266B nominal position (marked with a *cross*), as derived from timing (see P03). An accurate photometric analysis has been carried out for all the ~ 25 stars found in our catalog within a distance of $1\overset{''}{.}2$ from the PSR 6266B position. This correspond to ≤ 3 times the radius ($0".5$) of the circle accounting for the 1σ uncertainty in the absolute astrometry of the HST data. In particular, we have extracted 19 individual images from our dataset (10 exposures with ACS and 9 with WFPC2 camera) and compared the resulting magnitudes for each object in order to search for variability and estimate the typical photometric uncertainties for different classes of magnitude. Only one source in the catalog (hereafter named COM 6266B, marked with a small circle in Fig. 4.4) showed H_α variability ($\Delta H_\alpha \sim 0.2$ mag) significantly larger than the typical rms magnitude fluctuations ($\delta H_\alpha \sim 0.02$ mag in ACS data, and $\delta H_\alpha \sim 0.04$ mag in WFPC2 data) of stars of similar luminosity. Its celestial coordinates are $\alpha_{\rm J2000} = 17^{\rm h}01^{\rm m}12^{\rm s}.690$ and $\delta_{\rm J2000} = -30°06'48\overset{''}{.}61$ whereas the mean apparent magnitudes are B=20.58, V=19.48, R=19.02, $H_\alpha = 18.65$ (V is from Beccari et al. 2006). It is located just at the edge of the positional error circle for PSR 6266B. Fig. 4.3 reports the $(R, H\alpha - R)$ and $(R, B - R)$ Color Magnitude Diagrams (CMDs) for all the stars detected in the $20" \times 20"$ box centered on the PSR 6266B nominal position. COM 6266B is marked with a *large filled triangle* in both the CMDs. As apparent from the Figure the star has almost the same luminosity of the cluster Turn Off, but it shows an anomalous red color which locates it out of the Main Sequence. The

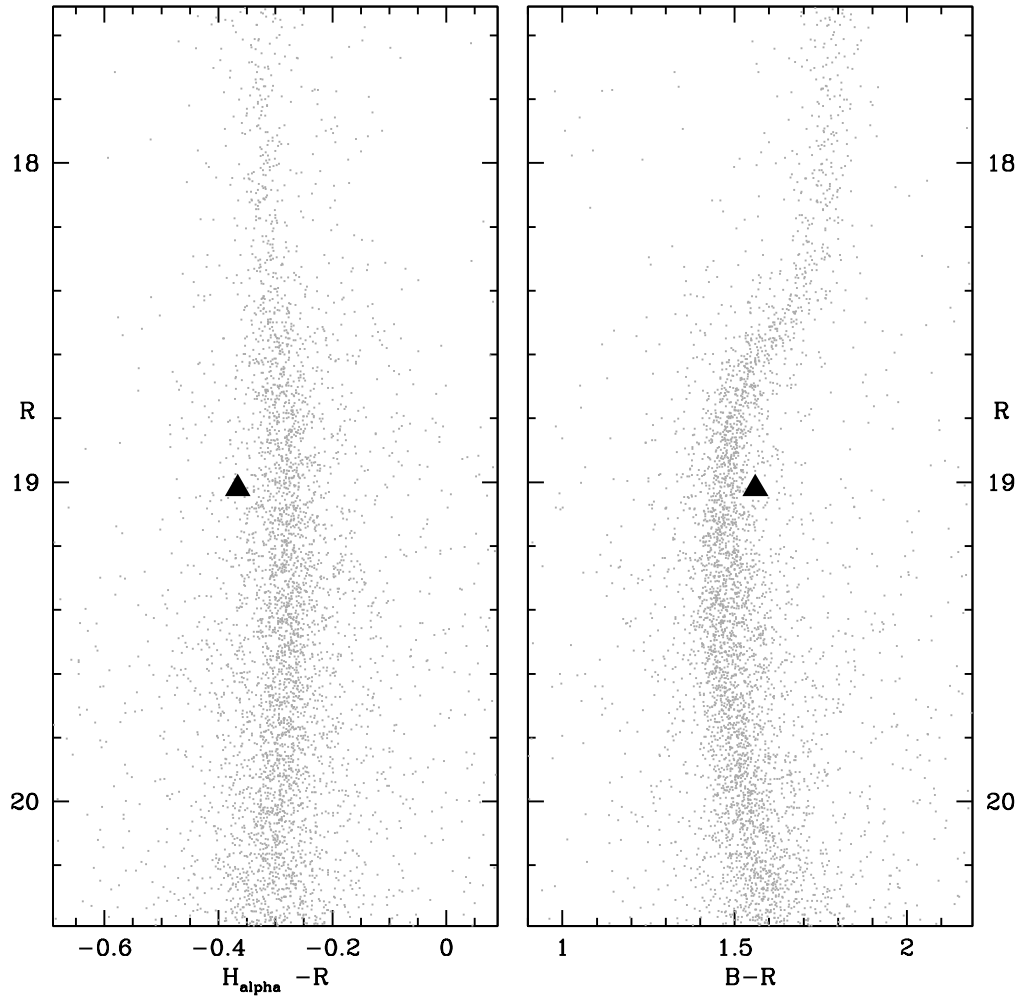

Figure 4.3: $(B, B - H_\alpha)$ and $(R, B - R)$ CMDs for the stars identified in a region of 20×20 centered at the nominal position of the . The optical counterpart to the pulsar companion is marked with a *large filled triangle*.

photometric properties imply that it is not a degenerate star and that it has a moderate $H\alpha$ excess (see Fig. 4.3), indicating the presence of ionized gas surrounding the system. These findings are consistent with the irregulaties seen in the radio signal of PSR 6266B and supports the scenario that COM 6266B is a mass loosing star. In order to firmly assess the physical connection between COM 6266B and the binary pulsar PSR 6266B, we have accurately investigated the time scale of the optical variability[5]. The H_α time series (19 points) was processed using GRATIS χ^2 fitting routine, a code developed at the Bologna Astronomical Observatory in order to study the periodicity of variable stars (see, e.g., Clementini et al. 2000). Following the procedure fully described in Ferraro et al. (2001), the most significant (99% confidence interval) periodicity was found at a period of 0.1446 ± 0.0015 day, consistent, within the uncertainties, with the orbital period of PSR 6266B derived from timing ($P_b = 0.1445454303(6)$ day, where the figure in parenthesis is the uncertainty, at 99% confidence level, on the last quoted digit; P03). Given that, we have folded the 19 magnitude values using P_b and the reference epoch of the PSR 6266B radio ephemeris ($T_0 = 52047.258199(2)$; P03).The results are shown in Fig.4.5. As apparent, the ACS and the WFPC2 data (obtained about 3 years later) agree with each other, defining a well defined light curve with two distinct maxima at about $\phi = 0.0$ and $\phi = 0.5$. This fact, as well as the phases and the amplitudes of the minima, confirm that the optical modulation is associated to the pulsar binary motions and strongly suggest that COM 6266B is a deformed star overflowing its Roche lobe.

Additional properties of this system can be derived from the analysis of the *Chandra* data. We found an X–ray source located at only $\sim 0".4$ from COM 6266B and at $0".3$ from the nominal radio position of PSR 6266B. The derived coordinates of the X-ray source are $\alpha_{\rm J2000} = 17^{\rm h}01^{\rm m}12^{\rm s}.696$ and $\delta_{\rm J2000} = -30°06'49".06$, and the 1σ uncertainty area on its position is encircled in Fig.4.4 (dashed line). Given the number of sources (50) detected within the half-mass radius of NGC 6266, the probability of a chance

[5]Note that COM 6266B has a close companion located at only 4 pixels ($\sim 0\overset{''}{.}19$) West in the ACS map (see Fig.4.4). This object turns out to be a normal Sub-Giant Branch star, slightly brighter (~ 0.5 mag in B, R and H_α) than COM 6266B and not displaying any evidence of variability. Although very close to each other, the two stars are clearly separable in the high resolution ACS and WFPC2 images and we have verified that the photometric analysis of COM 6266B is not affected by the presence of this close star.

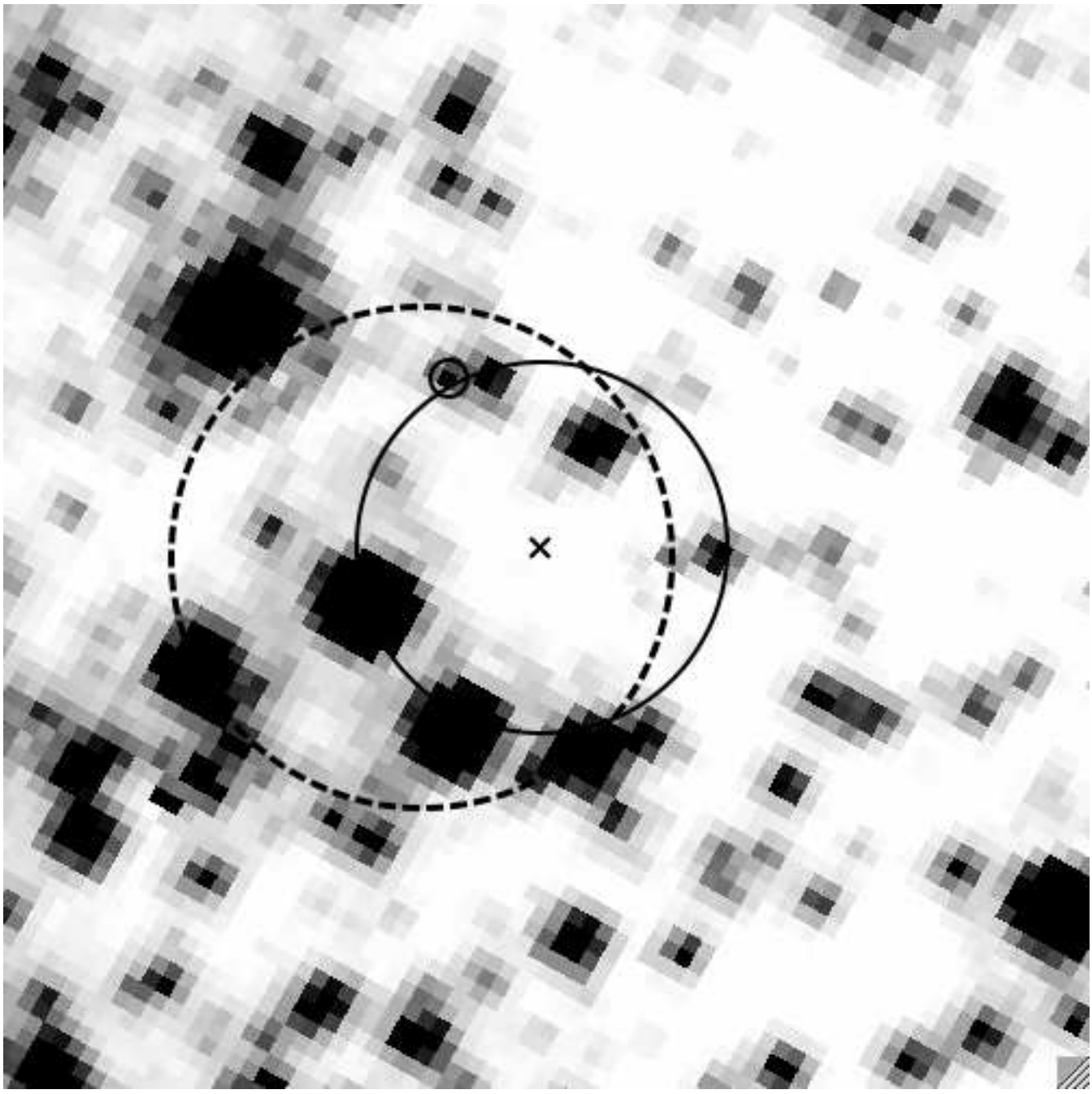

Figure 4.4: Finding chart for showing the median-combined $H\alpha$ image. The region covers 2×2; the cross marks the nominal position of PSR$-$B,with the 1σ error circle (05, solid line). The smaller circle shows the optical counterpart, whereas the dashed circle represent the 1σ in the *Chandra* position. North is up and East is to the left.

superposition of an X–ray source within $0\overset{''}{.}3$ from the radio position of PSR 6266B is $\sim 7\times10^{-4}$, strongly supporting the association of the detected source with the PSR 6266B system. The (background substracted) photons counts are $18.3^{+5.3}_{-4.2}$ (soft: 0.2-1 keV), $23.7^{+6.0}_{-4.9}$ (medium: 1-2 keV) and $9.8^{+4.3}_{-3.1}$ (hard: 2-8 keV), implying $H1 \simeq 1.3$ and $H2 \simeq 0.4$ (where HR1=medium/soft counts and HR2=hard/medium counts). Hence the source is harder than the typical MSPs population observed in GCs (e.g. Grindlay et al. 2002) and HR1, HR2 resemble those of a source in which the pulsar wind shocks the material released from the companion (see, e.g., the cases of PSR J1740−5340 in NGC 6397, and PSR J0024−7204W in 47Tuc; Grindlay et al. 2002, and Bogdanov et al. 2005, respectively). Even if the small number of photons prevents a detailed spectral analysis, for an absorption column density $N_H = 2.2 \times 10^{-21}\,\mathrm{cm}^{-2}$ (Pooley et al. 2003), the counts in each band and the HR1 and HR2 values are consistent[6] with a power law model having a photon index $\simeq 2.5$, and a total unabsorbed flux $F_X \sim 10^{-14}\,\mathrm{erg\ cm^{-2}sec^{-1}}$ in the 0.2-8 keV band, translating (for a distance of 6.6 kpc; Beccari et al. 2006) into a X–ray luminosity of $L_X \sim 6 \times 10^{31}\,\mathrm{erg\ sec^{-1}}$.

4.4 Discussion

Many observed features of COM 6266B (namely, its anomalous red colour, the H_α excess, the shape of the light curve, the X-ray emission from the binary) are suggestive of a tidally deformed star, which is experiencing heavy mass loss, similar to the system found in NGC 6397 by Ferraro et al. (2001). On the other hand, other photometric properties of the source does not fit in this picture, as described below. The comparison of the position of COM 6266B in the CMDs (Fig. 4.3) with the isochrones by Pietrinferni et al. (2004) (adopting [Fe/H]=-1.1 and an age of 12 Gyr for NGC6266) results in an effective temperature $T_{\rm eff} \sim 6000 \pm 500$ K and a bolometric luminosity $L_{\rm bol} \sim 1.9 \pm 0.2\ \mathrm{L}_\odot$, for extinction and distance like in Beccari et al. 2006. The implied emission radius[7] is

[6]The PIMMS tool has been used for these estimates: `http://heasarc.gsfc.nasa.gov/Tools/w3pimms.html`

[7]The uncertainties in $T_{\rm eff}$, $L_{\rm bol}$ and $R_{\rm em}$ account for both the flux and color variations of COM 6266B and the uncertainties in the distance, in extinction and in matching the CMDs with the isochrones.

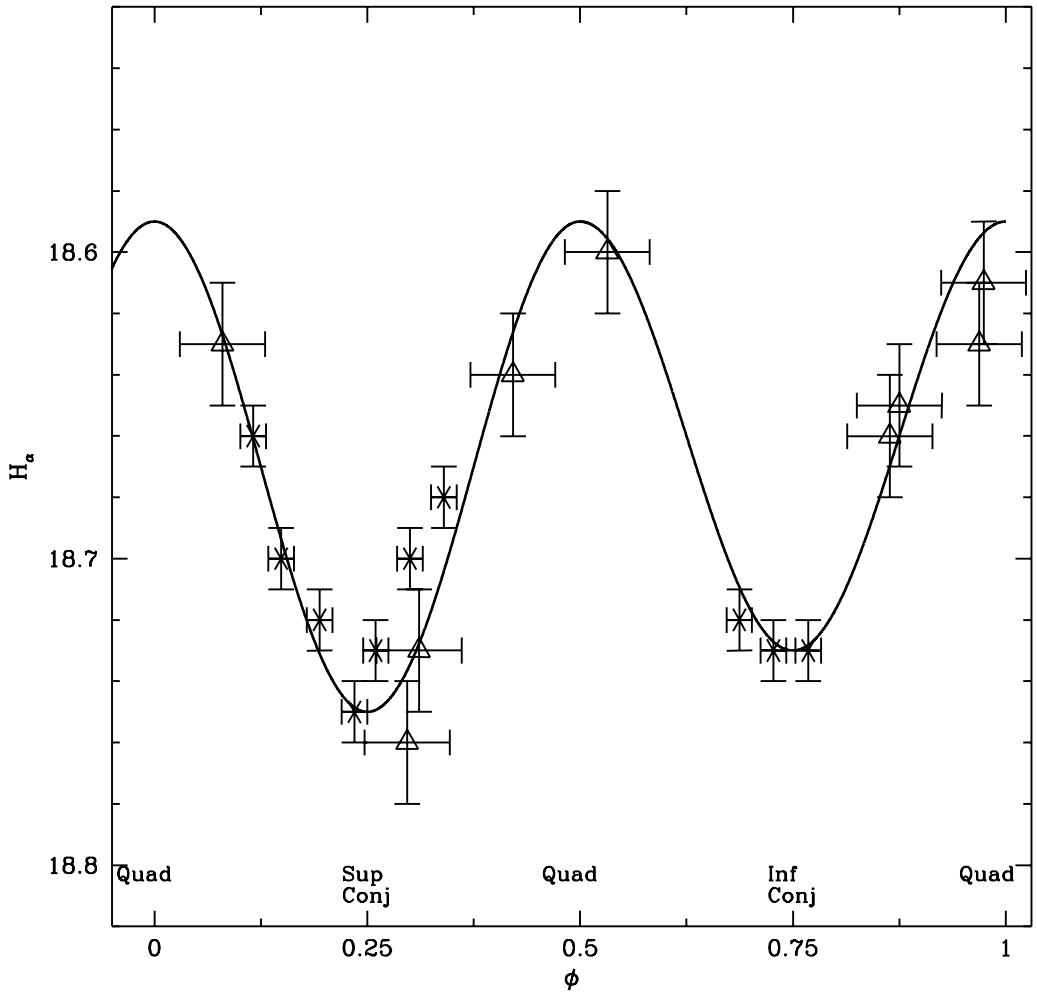

Figure 4.5: Ligh curve of in the H_α obtained by using the period and the reference epoch of the radio ephemeris of . Asterisks represent ACS archive observations performed in August 2004; large empty triangles are the WFPC2 data collected in May 2007. The phases of quadrature and conjunction of are reported for clarity. The *Solid Line* represent the Fourier ime series (truncated to the second harmonic) that best fits the data.

$R_{\rm em} \sim 1.2 \pm 0.2$ R$_\odot$. If the luminosity variations shown in Fig. 4.5 are mainly due to tidal deformations, $R_{\rm em}$ is expected to be of the order of the Roche lobe radius $R_{\rm rl}$ of the companion. The latter can be estimated from the mass function and projected semi-major axis of PSR 6266B (derived from pulsar timing, P03), provided a pulsar mass $M_{\rm psr}$ and an orbital inclination i are assumed. As already discussed in P03, the presence of radio eclipses indicates that i is not small[8]. Conservately taking $i \gtrsim 20^\circ$ and assuming $M_{\rm psr} = 1.4$ M$_\odot$, the companion star is expected to span the mass interval from 0.125 M$_\odot$ ($i = 90^\circ$) to 0.41 M$_\odot$ ($i = 20^\circ$), corresponding to $R_{\rm rl} \sim 0.26 - 0.40$ R$_\odot$. The upper value of $R_{\rm rl}$ is only slightly affected by the choice of $M_{\rm psr}$, being $R_{\rm rl} \lesssim 0.45$ R$_\odot$ for 0.7 M$_\odot \leq M_{\rm psr} \leq 3.0$ M$_\odot$, a safely large neutron star mass range (see e.g. Freire et al. 2008). In summary, for all plausible binary parameters, it turns out $R_{\rm em} \gtrsim 3\ R_{\rm rl}$. In order to match $R_{\rm em}$ with $R_{\rm rl}$ it should be $i \sim 3\,{\rm deg}$ (for $M_{\rm psr} = 1.4$ M$_\odot$) implying an unreliable companion mass ~ 6 M$_\odot$. In the hypothesis that COM 6266B is the companion to PSR 6266B, which is the origin of this discrepancy? A number of possibilities are examined below.

(i) The binary system does not belong to the cluster. This could easily lead to reconcile $R_{\rm em}$ with $R_{\rm rl}$. On the other hand, the celestial position of PSR 6266B is at less than 2 from the cluster center, and the pulsar shows a negative value of the spin period derivative, as expected if PSR 6266B lies in the cluster potential well.

(ii) The optical luminosity is dominated by strong non-thermal processes, maybe triggered by the pulsar spin down power $L_{\rm sd}10$ L$_\odot$ (see P03). In this case, a large disagreement between $R_{\rm em}$ (evaluted from $L_{\rm bol} = 4\pi R_{\rm em}^2 \sigma_B T_{\rm eff}^4$, with σ_B the constant of Stefan-Boltzmann) and $R_{\rm rl}$ may be expected. However, it is hard to explain how a large non-thermal component may generate a light curve whose maxima fall at orbital phases which nicely fit with typical ellipsoidal variations.

(iii) COM 6266B is the blending of two stars. This is not uncommon in the crowded stellar field of a GC core. One star would be the optically variable companion to PSR 6266B and the other star a not variable star in the foreground (background).

[8]This is also an implicit consequence of the hypothesis that the shape of the light curve is due to ellipsoidal variations, the modulation of which tends to vanish for small values of i.

However this only partially alleviates the problem. E.g. assuming that the luminosity of COM 6266B comes from two stars of equal mean H_α magnitude (i.e. $H_\alpha = 19.35$ mag), the observed ellipsoidal modulation could only be produced if the modulation of the light curve of the pulsar companion reaches $\Delta m_{\mathrm{H}_\alpha} \sim 0.35$ mag, a rather extreme value for this kind of variable stars. Even in this case, we are left with an emission radius $R_{\mathrm{em}} 1.7 R_{\mathrm{rl}}$. Matching R_{em} with R_{rl} would require that COM 6266B is the blend of a not variable star with $H_\alpha = 18.8$ mag and a star of mean magnitude $H_\alpha = 20.6$ mag and having $\Delta m_{\mathrm{H}_\alpha} \sim 2$ mag. We note that similar considerations would apply if PSR 6266B were a triple system.

Options *(i)* and *(ii)* will be finally addressed as soon as spectroscopic data will be available for the system, allowing to investigate its association to the cluster (via determination of the radial velocity) and the nature of its optical spectrum.

Chapter 5

Conclusion

The optical detection of the companion to a binary MSP is fundamental to understand the origin and the evolution of this kind of binary systems. For those systems harbored in a GC, the analysis of the MSP companions is also more important, because it can be very helpful in the investigations of the dynamical interactions that can take place in a GC. Despite several efforts in the last years, observational progresses in detecting optical counterparts of cluster binary MSPs are quite slow (up to now only six of such counterparts were identified), mainly because of the high spatial resolution needed and sensitivity limitations.

The first two detections of MSP companion in a GC was $U_{\rm opt}$, the companion to PSR J0024−7203U and the faint and blue source W29, the companion to the MSP PSR J0024−7204W, both in 47 Tuc (Edmonds et al., 2001, 2002); comparing the position of $U_{\rm opt}$ in a Color Magnitude Diagram with theoretical models these authors are shown that this star is a low-mass ($\lesssim 0.17 M_{\odot}$) Helium White Dwarf. A little bit more massive ($M_c = 0.28\,{\rm M}_{\odot}/{\rm sini}$) white dwarf has been found orbiting around PSR B1620-26 in the Globular Cluster M4 (Sigurdsson et al., 2003): this pulsar possesses an anomalously large second time derivate of the rotational period and further radio observations reveled the third and fourth derivatives of the pulsar period as well as a secular change in the projected semimajor axis of the inner binary. On the basis of these contraints, Sigurdsson et al. (2003) proposed a model in which a third body (=a planet) is responsable for the observed time varying acceleration.

In this work we have presented the properties of two MSP companion: in the chapter

§3 we showed the spectroscopical and photometrical properties of COM J1911−5958A in the Globular Cluster NGC6752. This object turn out to be a low mass ($\simeq 0.18 M_{\odot}$) Helium White Dwarf, as aspected from the recycling scenario. A very peculiar carachteristic of this object is the anomalous position respect to center of mass (or gravity) of the cluster: radial velocity measurment are shown that COM J1911−5958A belongs to NGC6752, despite it is located more than $6'$ from the cluster center. The scenario proposed from Colpi et al.(2003) suggests that a strong interaction occured in the cluster core: considering that dynamical friction could rapidly drive back to the cluster core an object of total mass of order 1.6 $M_{\odot}$, the ejection of PSR J1911−5958A from the core to the outskirts of NGC 6752 (implying a radial orbit) cannot be occurred more than $\tau_{\rm df} = 0.7 \div 1$ Gyr ago. On the other hand the cooling age of COM J1911−5958A is longer than $\tau_{\rm df}$, implying that any dynamical event responsible for the ejection, probably acted on an already recycled millisecond pulsar. Despite this is an *ad hoc* hypotesis, a binary black hole of mass in the range $100 \div 200\,{\rm M}_{\odot}$ could be a plausible candidate: the same idea may also expalains the anomalous acceleration along the line of sight of at least two out of three MSP hosted in the cluster core. Recent works have also shown that small deviation from classical shape of the surface brightness in globular clusters with a suspected collapsed core (see for example Baumgart et al., 2005, Trenti et al. 2007) may be interpreted as the signature of the presence of an intermediate mass black hole: in this framework also the status of the core of NGC6752, could suggest the presence of an IMBH in this cluster. Many authors (see the discussion in chapter 3) found in fact that the core of this cluster shows small deviation from the classical King-model profile.

Altought this is still a very controversial subject, NGC6752 is one of the few globular cluster in which the presence of an IMBH is suspected (Miocchi et al., 2007)

Another peculiar caracteristic of the COM J1911−5958A is the puzzling light curve, showing two maxima at orbital phases 0.05 and 0.5; modulation of the optical light curve of the companion to a MSP may occured in the case of the heating of one emisphere of the star (whose rotation is syncronized with the orbital period) due to the radiation coming from the pulsar, but in the case of COM J1911−5958A the irradiation coming from the pulsar should be negligible.

Ellipsoidal modulation due to the tidal deformation of the companion are known to produce a light curve with two peaks at quadratures (see for example the case of PSR J1701−3006 in NGC 6266 described in the chapter 4 of this work) but tidal deformations are expected to be insignificant for a companion whose radius is ~ 20 times smaller than the radius of its Roche lobe.

The optical modulation can be intrinsic to the He-WD, in the framework of an oblique rotator model for the WD, in which photometric modulations have been interpreted with changes with the rotational phase of the mean magnetic field.

In the chapter 4 we have presented the discovery of the sixth companion of a MSP in a globular cluster, COM J1701−3006 in NGC 6266. This object turn out to be a bright star with an anomalous red color and optical variability ($\sim 0.2mag$) nicely correlates to the orbital period of the pulsar. The shape of the optical light curve is a clear signature of tidal distortion, suggesting that the MSP companion is a bloated star, completely filling its Roche Lobe; this star also lies within the error box position of a low luminosity $L_x \simeq 6 \times 10^{31} ergs^{-1}$ and quite hard X-ray sources, supporting the hypotesis that some interaction is occurring between the pulsar wind and the gas streaming off the companion. This is the second case in which such an object has been found to orbits a MSP in a globular cluster (being COM J1740−5340 the first, Ferraro et al. 2001b), suggesting that these kind of systems could represent an intermediate evolutionary stage of the recycling process, or the result of a more recent exchange interaction with a MS star occurred in the cluster core. Comparing the position of the COM J1701−3006 in the CMD with theoretical isochrones, we found that the radius of the star ($R \gtrsim 1R_{\odot}$) deduced from the luminosity and the temperature ($L \sim 1.9L_{\odot}$ and $T \sim 6000K$) is three times larger of the Roche Lobe of the star. Possible explanation for this mismatch are also discussed a the end of chapter 4: the presence of a third companion or the blend of two stars in the crowded field of NGC6266 could alleviate the problem, as well as the occurrence of non thermal processes, maybe triggered by the spin down power of the pulsar. Both these hypotesis can affected the optical luminosity of COM J1701−3006, leading to overstimate the radius of the star, calculeted from the classical formula $L_{\rm bol} = 4\pi R_{\rm em}^2 \sigma_B T_{\rm eff}^4$.

As also noted in the previous chapter, the optical and X-Ray properties of the

PSR 6266B system impressively resembles those PSR J1740−5340. On the other hand, P03 already noted that the radio emission of PSR−B displayed irregular eclipses near the superior conjunction, from phase $\sim$ 0.15 to phase $\sim$ 0.35, meaning that the eclipses are due to the matter overflowing the Roche lobe of the companion star. This kind of systems, formed with a recycled eclipsing radio pulsar and a relative massive ($M > 0.10 M_{\odot}$) companion, could be frequent in Globular Clusters, as emerging from recent surveys: PSR J0024− 7204U and PSR J0024− 7204W in 47 Tuc (Camilo et al., 2000), PSR J1748-2446A, PSR J1748-2446P and PSR J1748-2446ad in Terzan 5 (Ransom et al., 2005) and PSR J1740−5340 (Ferraro et al., 2001b; Grindlay et al., 2002) shows similar properties. As in the case of PSR J1740−5340 it is clear from its position on the CMD that PSR 6266B is not a WD. Evolutive computations, (Burderi D'Antona & Burgay, 2002),indicate that the companion star of PSR J1740−5340 will become an He-WD of $\sim 0.2\,\mathrm{M}_{\odot}$, assuming that the initial mass of the companion to the MSP was $M_2 = 0.85 M_{\odot}$ and the neutron star mass is $M_1 = 1.4\,\mathrm{M}_{\odot}$. If we assumed a similar scenario for PSR 6266B we may hypotize that COM 6266B will show photometric properties very similar to those of other He-WD orbiting around MSP as for example U_{opt} and COM J1911−5958A. Thus they could represent an intermediate/final stage of the recycling process, leading the formation of MSP/He-WD systems or systems with very low mass star orbiting a MSP. If further supported by additional cases, this evidences could confirm that a low mass $\sim 0.15 \div 0.2\,\mathrm{M}_{\odot}$ He-WD orbiting a MSP is the favored system generated by the recycling process of MSPs, not only in the Galactic field (Hansen & Phinney, 1998), but also in GCs (Rasio Pfahl & Rappaport, 2000).

As a part of the long term program started at the University of Bologna, new observation of other GCs, as for example Terzan 5, which hosts 33 MSP and 17 MSP in binary sistems, has been obtained by using HST, in the aim of double/triple the existing sample of known MSP companion, shedding light on thier formation and evolution mechanism.

Optical identification of a larger sample of MSP companion could allows a deep insight on the phisycal processes occurring in these binary systems. Carefull examination of the companion light curve , as induced for example by ellipsoidal distortion or by the

irradiation of the pulsar flux, may constrain the orbital parameters as well as investigate the effects of the irradiatiun flux of the MSP onto the companion surface. Moreover, the possibility to derive the mass ratio ratio of these systems from the radial velocity curve of the companion leads to a direct estimate of the pulsar mass. This is particulary interesting since the NS in these systems is expected to be more massive (due to the heavy mass accretion) than the canonical $1.35 \div 1.40 M_{\odot}$. The prediction on the maximum NS mass by different equation of state of the nuclear matter can be checked, demostrating the crucial role that MSP studies play in the fundamental problems of physics and astrophysics.

Bibliography

Bibliography

Alpar, M.A., Cheng, A.F., Ruderman, M.A., and Shaham, J. 1982, Nature, 300, 728

Aurière, M. & Ortolani, S. 1989, A&A, 221, 20 (AO89) S

Backer, D.C., Kulkarmi, S.R., Heiles C., Davis, M.M., Goss, W.M. 1982, Nature, 300, 615

Bailes, M. 1989, ApJ, 342, 917

Bassa, C.G., Verbunt, F., van Kerkwijk, M.H., & Homer, L. 2003, A&A, 409, L31

Baumgardt, H., Hut, P., Makino, J., McMillen, S., & Portegies Zwart S. 2003, ApJ, 582, L21

Baumgardt H., Makino J., Hut P. 2005, ApJ, 620, 238

Beccari, G., Ferraro, F. R., Possenti, A., Valenti, E., Origlia, L. and Rood, R. T. 2006 AJ, 131,2551B

Bergeron, P., Fontaine, G., Billères, M., Boudreault, S., & Green, E. M. 2004, ApJ, 600, 404

Bettwieser,E., & Sugimoto, D. 1984, MNRAS, 208, 439

Bhattacharya, D., & van den Heuvel, E.P.J. 1991, Phys. Rep., 203, 1

Bogdanov, S., Grindlay, J. E. and van den Berg, M. 2005, ApjL, 630 1029

Buonanno, R., Buscema, G., Corsi, C.E.,Ferraro, I., & Iannicola, G. 1983, A&A, 126, 278

Burderi, L., D'Antona, F., & Burgay, M. 2002, ApJ, 574, 325

Burgay, M., 2003, Nature

Callanan, P.J., van Paradijs J., & Rengelink R. 1995, ApJ, 439, 928

Camilo, F., Lorimer, D.R., Freire, P., Lyne, A.G., & Manchester, R.N. 2000, ApJ, 535, 975

Campana, S., Colpi, M., Mereghetti, S., Stella, L., & Tavani, M. 1998, A&A Rev., 8, 279

Carretta, E., Gratton, R., Clementini, G. & Fusi-Pecci, F. 2000, ApJ 533, 215

Chernoff, D.F., & Djorgowski, S.G. 1989, ApJ, 339, L904

Chernoff, D.F, & Weinberg, M.D. 1990, ApJ, 351, 121

Clark, G. 1975, ApJ, 199, L143

Clementini, G., et al. 2000, AJ, 120, 2054

Cocozza, G., Ferraro, F. R., Possenti, A., & D'Amico, N. 2006, ApjL, 641, L129

Cocozza, G., Ferraro, F. R., Possenti, A., Beccari, G., Lanzoni, B., Ransom, S., Rood, R.& D'Amico, N. 2008, ApJL submitted

Cohn, H. 1908, ApJ, 242, 765

Cohn, H., Lugger, P. M., Grabhorn, R.P., Breeden, J.L., Packard, N.H., Murphy, B.W., & Hut, P. 1991, in The Formation and Evolution of Star Clusters, ed K. Janes (San Francisco: ASP), 381

Colpi, M., Possenti, A., & Gualandris, A. 2002, ApJ, 570, L85

Colpi, M., Mapelli, M., & Possenti, A. 2003a, ApJ, 599, 1260

Colpi, M., Mapelli, M., & Possenti, A. 2003b, "Coevolution of Black Hols and Galaxies", Carnegie Observatories Astrophysics Series, Vol. 1: ed. L. C. Ho (Pasadena: Carnegie Observatories)

Corongiu, A., Possenti, A., Lyne, A. G., Manchester, R. N., Camilo, F., D'Amico, N. & Sarkissian, J. M. 2006 ApJ 653 141

D'Amico, N., Lyne, A.G., Manchester, R.N., Possenti, A., & Camilo, F. 2001a, ApJ, 548 L171

D'Amico, N., Possenti, A., Manchester, R.N., Sarkissian, J., Lyne, A.G. & Camilo, F 2001b, ApJ, 561, L89

D'Amico, N., Possenti, A., Fici, L., Manchester, R. N., Lyne, A.G., Camilo, F. & Sarkissian, J. 2002, ApJ, 570, L89

D'Antona, F. 1995, in *Evolutionary Processes in Binary Stars*, NATO-ASI Series, ed. R.A.M. Wijers, M.B. Davies, C.A. Tout, Kluwer, 287

Davies, M.B, Hansen, B.M.S 1998, MNRAS, 301, 15 4, MNRAS, 349, 129

Dinescu, D.I., Girard, T.M., van Altena, W.F., 1999, AJ, 117, 1792

Djorgovski, S. & King, I. R. 1986, ApJ, 305, L71 (DK86)

Djorgovski, S. 1993, in ASP Conf. Ser. 50, Structure and Dynamics of Globular Clusters, ed. S. G. Djorgovski & G. Meylan, (San Francisco: ASP), 373

Djorgovski, S.G., & Meylan, G. 1993, in ASP Conf. Ser. 50, Structure and Dynamics of Globular Cluster, ed. S. G. Djorgovski & G. Meylan (San Francisco, ASP), 325

Djorgovski, S., & Meylan, G. 1994, AJ, 108, 1292

Dolphin A.E., 2002 PASP, 112, 1383

Drukier, G.A. 1996, MNRAS, 280, 498

Drukier, G.A., Bailyn, C.D., Van Altena, W.F., Girard, T.M. 2003, AJ, 125, 2559

Dubath, P., Meylan G., & Mayor, M. 1997, A&A, 324, 505

Dull, J.D., Cohn, H.N., Lugger, P.M., Murphy, B.W, Seitzer, O.P., Callanan, P.J., Rutten, R.G, Charles, P.A. 1997, ApJ, 481, 267

Dull, J.D., Cohn, H.N., Lugger, P.M., Murphy, B.W, Seitzer, O.P., Callanan, P.J., Rutten, R.G, Charles, P.A. 2003, ApJ, 585, 598

Edmonds, P.D., Gilliland, R.L., Heinke, C.O., Grindlay, J.E., Camilo, F. 2001, ApJ, 557, L57

Edmonds, P.D., Gilliland, R.L., Camilo, F., Heinke, C.O., & Grindlay, J.E. 2002, ApJ, 579, 741

Edmonds, P.D., Gilliland, R.L., Heinke, C.O, & Grindlay, J.E. 2003, ApJ, 596, 1177

Fabian, A.C., Pringle, J.E., & Rees, M.J. 1975, MNRAS, 172, L15

Ferrario, L., Vennes, S., Wickramasinghe, D. T., Bailey, J. A., & Christian, D. J. 1997, MNRAS, 292, 205 ni, M. 1995 A&A, 294, 80

Ferraro, F.R., Paltrinieri, B., Fusi Pecci, F., Cacciari, C., Dorman, B., Rood, R.T., Buonanno, R., Corsi, C. E., Burgarella, D., Laget, M., 1997a, A&A, 324, 915

Ferraro, F.R., Carretta, E., Bragaglia, A., Renzini, A., Ortolani, S. 1997b, MNRAS, 286, 1012

Ferraro, F.R., Paltrinieri, B., Rood, R.T., Dorman, B. 1999a, ApJ, 522, 983

Ferraro, F.R., Messineo, M., Fusi Pecci, F., de Palo, M.A., Straniero, O., Chieffi, A., Limongi, M. 1999b, AJ, 118, 1783

Ferraro, F.R., Paltrinieri, B., & Cacciari, C. 1999a Mem SAIt, 70, 599

Ferraro, F.R., D'Amico, N., Possenti, A., Mignani, R., & Paltrinieri, B. 2001a, ApJ, 561, 337

Ferraro, F.R., Possenti, A., D'Amico, N. & Sabbi, E. 2001b, ApJ, 561, L93

Ferraro, F.R., Possenti, A., Sabbi, E., Lagani, P., Rood, R.T., D'Amico, N., & Origlia, L 2003a, ApJ, 595, 464

Ferraro, F.R., Sabbi, E., Gratton, R.G., Possenti, A., D'Amico, N., Bragaglia, A., & Camilo, F. 2003b, ApJ, 584, L13

Ferraro, F.R., Sills, A., Rood, R.T., Paltrinieri, & B., Buonanno, R. 2003c, ApJ, 588, 464

Ferraro, F.R., Beccari, G., Rood, R.T., Bellazzini, M., Sills, A., Sabbi, E. 2004, ApJ, 603,127

Frank, J., King, A., & Raine, D. 2002, Accretion Power in Astrophysics, Cambridge University Press (thirdedition)

Freeman, P.E., Kashyap, V., Rosner, R., Lamb D.Q. 2002 ApJS 138 185

Fregeau, J.M., G*ü*rkan, M.A., Joshi, K.J., & Rasio, F.A. 2003, ApJ, 593, 772

Freire, P.C., Camilo, F., Lorimer, D.R., Lyne, A.G., Manchester, R.N., & D'Amico, N 2001a, MNRAS, 326, 901

Freire, P.C., Kramer, M., Lyne, A.G., Camilo, F., Manchester, R.N., & D'Amico, N 2001b, ApJ, 557, L105

Freire, P.C., Camilo, F., Kramer, M., Lorimer, D.R., Lyne, A.G., Manchester, R.N., & D'Amico, N. 2003, MNRAS, 340, 1359

Fruchter, A.S., et al. 1990, ApJ, 351, 642

Gerssen, J., van der Marel, R.P., Gebhardt, K., Guhathakurta, P., Peterson, R. C., & Pryor, C. 2003, AJ, 125, 376

Giacconi, R., Murray, S., Gursky, H., Kellogg, E., Schreier, E., Matilsky, T., Koch, D. & Tananbaum, H., 1974, ApJ 27, 37

Goodman, J. 1989, “Dynamics of Dense Stellar Systems”, ed. D. Merritt, Cambridge: Cambridge Unv. Press

Grabhorn, R.P., Cohn, H.N., Lugger, P.M., & Murphy, B.W. 1992, ApJ, 392, 86

Gratton, R., Bragaglia, A., Carretta, E., Clementini, G., Desidera, S., Grundhal, F & Lucatello, S. 2003, A&A, 408, 529

Gratton, R., Sneden, C., & Carretta, E. 2004, ARA&A, 42, 385

Grindlay, J.E., Hertz, P., Steiner, J.E., Murray, S.S.,Lightman, A.P. 1984, ApJ,282,L13

Grindlay, J.E.,Cool, A.M, Callanan, P.J., Bailyn, C.D., Cohn, H.N., & LuggerP.M., 1995, ApJ, 581, 470

Grindlay, J.E., Heinke, C.O., Edmonds, P.D., Murray, S.S.& Cool, A. 2001a, ApJ, 563, L53

Grindlay, J.E., Heinke, C., Edmonds, P.D., & Murray, S.S. 2001b, Science, 292, 2290

Grindlay, J.E., Camilo, F., Heinke, C.O., Edmonds, P.D., Cohn, H., & Lugger, P. 2002, ApJ, 581, 470

Guenther, D.B., Demarque, P., Kim, Y.C., & Pinsonneault, M.H. 1992, ApJ, 387, 372

Hansen, B.M.S., & Phinney, E.S. 1998, MNRAS, 294, 569

Harris, W.E. 1987, PASP,99.1031

Harris, W.E. 1996, AJ, 112, 1487

Heggie, D.C. 1975, MNRAS, 173, 729

Heinke, C. O., Wijnands, R., Cohn, H. N., Lugger, P. M., Grindlay, J. E., Pooley, D. & Lewin, W. H. G. 2006 ApJ 651 1098

Heńon, M. 1961, Ann. Astrophyr., 24, 369

Hertz, P., & Grindlay, J.E. 1983,ApJ, 275, 105

Hessels, J.W.T., Ransom, S.M. Stairs, I.H. Freire, P.C.C., Kaspi, V.M. & Camilo, F. Science 640, 428

Hills, J.G., & Day, C.A. 1976 ApJ, 17, L87

Hills, J.G. 1983, ApJ, 267, 322

Holtzmann, J.A., Burrows, C.J., Casertano, S., Hester, J.J., Trauger, J.T., Watson, A.M., & Worthey, G. 1995, PASP, 107, 1065

Hurley, J.R., & Shara, M.M. 2002, ApJ, 570, 184

Hulse, R.A., Taylor, J.H. 1975 ApJL, 195, 51

Hut, P. & Verbunt, F. 1983 Nature, 301, 508

Hut, P., & Djorgovski, S. 1982, Nature, 257, 513

Hut, P., McMillan, S., Goodman, J.C., Mateo, M., Phinney, E.S., Pryor, C., Richer, H.B., Verbunt, F., & Weinberg, M. 1992, PASP, 104, 981

Katz, J.,I., 1975 Nature 253, 698

King, I.R. 1966, AJ, 71, 64

King, I.R., Sosin, C., & cool, A. 1995, ApJ, 452, L33

Knigge, C., Zurek, D.R., Shara, M.M., & Long, K.S. 2002, ApJ, 579, 725

Kong, A.K.H., Bassa, C., Pooley, D., Lewin, W.H.G,; Homer, L., Verbunt, F., Anderson, S.F., Margon, B. 2006 ApJ 647 1065

Kurucz, R.L. 1995, CD-ROM 13, Opacities for Stellar Atmospheres: Abundance Sample (Cambridge: Smithsonian Astrophys. Obs.)

Landolt, A.U. 1992, AJ, 104, 340

Leonard, P.J.T. & Livio, M. 1995, ApJ 447, L121

Lightman, A. 1982, ApJ, 263, L19

Livio, M. 1993, in Blue Stragglers, ASP Conference Series, ed. Saffer, R.A., (San Francisco:ASP), 53, 3

Lombardi, J.C., Rasio, F.A., & Shapiro, S.L. 1995, ApJ, 445, L117

Lombardi, J.C., Rasio, F.A., & Shapiro, S.L. 1996, ApJ, 468, 797

Lorimer, D.R., Camilo, F., Freire, P., Kramer, M., Lyne, A.G., Manchester, R.N. — D'Amico, N. 2003, ASPC 302, 363

Lugger, P.M., Cohn, H.N. & Grindlay, J.E. 1995, ApJ, 439, 191 (LCG95)

Lynden-bell, D. & Wood, R. 1968 mnras 138, 495

Lynden-Bell, D., & Eggleton, P. 1980, MNRAS, 191, 483

Lyne, A.G., Biggs, J.D., Brinklow, A., McKenna, J., & Ashworth, M. 1988, Nature, 332, 45

Lyne, A.G., Johntson, S., Manchester, R.N., Staveley-Smith, L., & D'Amico, N. 1990, Nature, 347, 650

Lyne, A.G., Burgay, M., Kramer, M., Possenti, A., Manchester, R.N., Camilo, F., McLoughlin, M., Lorimer, D.,R., Joshi, B.C., Reynolds,J.E. & Freire, P.C.C. 2004 Science, 303, 1153

Manchester, R.N., Lyne, A.G., Robinson, C., Bailes, M., & D'Amico, N. 1991, Nature, 352, 219

Mapelli, M., Sigurdson, S., Colpi, M., Ferraro, F.R., Possenti, A., Rood, R.T., Sills, A., & Beccari, G. 2004, ApJ, 605, L29

McKenna, J., Lyne, A.G. 1988 Nature, 336, 226

Meylan, G. & Heggie, D.C. 1997, A&ARV, 8, 1

Miocchi, P., 2007, MNRAS 381, 103

Momany, Y., et al. 2001, A&A, 379, 436

Montegriffo, P., Ferraro, F.R., Fusi Pecci, F. & Origlia. L. 1995, MNRAS, 276, 739

Montes, D., Fernández–Figueroa, M.S., De Castro, E., & Sanz–Forcada, J. 1997, A&AS, 125, 263

Montes, D., Fernández–Figueroa, M.S., De Castro, E., Cornide, M., Latorre, A., & Sanz–Forcada, J. 2000, A&AS, 146, 103

Nemec, J.M., Harris, H.C. 1987, ApJ, 208, L55

Nice, D.J., & Thorsett, S.E. 1992, ApJ, 397, 249

Nice, D.J., Arzoumanian Z., & Thorsett, S. 2000, in IAU Colloq. 177, Pulsar Astronomy—2000 and Beyond, ed. M. Kramer, N. Wex, & R. Wielebinski (San Francisco: ASP), 67

Orosz, J.A., & van Kerkwijk, M.H. 2003, A&A, 397, 237

Pacini, F. 1967, Nature 216, 567

Pietrinferni, A., Cassisi, S., Salaris, M. & Castelli, F. 2004 ApJ 612 168

Phinney, E.S. 1992, Nature, 358, 198

Podsiadlowski, P. 1991, Nature, 350, 136

Podsiadlowski, P., Rappaport, S., & Pfahl, E. 2002, ApJ, 565, 1107

Pooley, D., et al. 2002, ApJ, 569, 405

Pooley, D., Lewin, W. H. G., Anderson, S. F., Baumgardt, H., Filippenko, A. V., Gaensler, B. M., Homer, L., Hut, P., Kaspi, V. M., Makino, J., Margon, B., McMillan, S., Portegies Zwart, S., van der Klis, M. and Verbunt, F. 2003 ApJL, 591, 131L

Pooley, D., & Hut, P. 2006 ApJ, 646, L143

Possenti, A. 2002, Neutron Stars Pulsars and Supernova Remnants, eds. W. Becker, H. Lesch & J. Trümper, MPE Report 278, p. 183

Possenti, A., D'Amico, N., Manchester, R. N., Camilo, F.,Lyne, A. G.,Sarkissian, J., Corongiu, A. 2003 ApJ, 599, 475P

Pryor, C. & Meylan, G. 1993, ASP Conf. Ser. 50: Structure and Dynamics of Globular Clusters, 357

Ransom, S.M., Hessels, J.W.T., Stairs, I.H., Freire, P.C.C., Camilo, F., Kaspi, V.M., Kaplan, D.L. 2005, Science, 307, 892

Rasio, F.A., Shapiro, S.L., & Teukolsky, S.A. 1991, A&A, 241, L25

Rasio, F.A., Pfahl, E.D., & Rappaport, S. 2000, ApJ, 532, L47

Ratnatunga, K.U., & Bahcall, J.N. 1985, ApJS, 59, 63

Renzini, A. 1983, Mem. Soc. Astron. Ital., 54, 335

Renzini, A., & Buzzoni, A. 1986, in Spectral Evolution of Galaxies, ed. C. Chiosi & A. Renzini (Dordrecht: Reidel), 135

Renzini, A., Bragaglia, A., Ferraro, F.R., Gilmozzi, R., Ortolani, S., Holberg, J.B., Liebert, J., Wesemovel, F., & Bohlin, R.C. 1996, ApJ, 465, L23

Robinson, C.R., Lyne,A.G., Manchester, A.G., Bailes, M., D'Amico, N., & Johnston, S. 1995, MNRAS, 274, 547

Rubenstein, E.P., & Bailyn, C.D. 1997, ApJ, 474, 701

Ruderman, M., Shaham, J., & Tavani M. 1989, ApJ, 336, 507

Russell, H.R. 1945, ApJ, 102, 1

Ryan, S.G., Beers, T.C., Kajino, T., & Rosolankova, K. 2001, ApJ, 547, 231

Sabbi, E., Gratton, R.G., Bragaglia, A., Ferraro, F.R., Possenti, A, Camilo, F., & D'Amico, N. 2003a, A&A 412, 829

Sabbi, E., Gratton, R.G., Ferraro, F.R., Bragaglia, A., Possenti, A, D'Amico, N., & Camilo, F. 2003b, ApJ, 589, L41

Sabbi, E., Ferraro, F.R., Sils, A., & Rood, R.T. 2004, ApJ, 617, 1296

Serenelli, A.M, Althaus, L.G., Rohrmann, R.D., & Benvenuto, O.G. 2001, MNRAS, 325, 607

Serenelli, A.M., Althaus, L.G., Rohrmann, R.D., & Benvenuto, O.G. 2002, MNRAS, 337, 1091

Shapiro, S.L., Teukolski, S.A. 1983, Black holes, white dwarfs, and neutron stars: The physics of compact objects, New York, Wiley-Interscience

Shapley, H. 1918, ApJ, 48, 154

Shara, M.M., Saffer, R.A., & Livio, M, 1997, ApJ, 489, L59

Shara, M.M., Saffer, R.A., & Livio, M. 1997, ApJ, 474, 701

Shara, M.M. 2002, ASP Conf. Ser. 263: "Stellar Collisions, Mergers and their Consequences"

Shvartsman, V. F. 1970, Radiofizika, 13, 1852

Siess, L., & Livio, M. 1999, MNRAS, 308, 1133

Sigurdsson, S., Davies, M.B., & Bolte, M. 1994, ApJ, 431, L115

Sigurdsson, S., & Phinney, E. S. 1995, ApJS, 99, 609

Sigurdsson, S. 2003, ASP Conf. Ser., 302, 391

Sigurdsson, S. Richer, H.B., Hansen, B.M., Stairs I.H., & Thorsett, S.E. 2003, Nature, 301, 193

Sills, A., Lombardi, J. C. Jr. 1997, ApJ, 484, L51

Sills, A., Lombardi, J. C., Bailyn, C. D., Demarque, P., Rasio, F. A., & Shapiro, S. L. 1997, ApJ, 487, 290

Sills, A., Bailyn, C. D. 1999, ApJ, 513, 428

Sills, A., Bailyn, C. D., Edmonds, P. D., Gilliland, R. L. 2000, ApJ, 535, 298

Sills, A., Faber, J. A., Lombardi, J. C., Rasio, F. A., & Warren, A. R. 2001, ApJ, 548, 323

Sills, A., Adams, T., Davies, M. B., & Bate, M. R. 2002, MNRAS, 332, 49

Silvestri, F., Ventura, P., D'Antona, F., & Mazzitelli, I. 1998, ApJ 509, 192

Sirianni, M.,Jee, M. J., Benítez, N., Blakeslee, J. P., Martel, A. R., Meurer, G., Clampin, M., De Marchi, G., Ford, H. C., Gilliland, R., Hartig, G. F., Illingworth, G. D., Mack, J. and McCann, W. J. 2005, PASP, 117, 1049

Smarr, L.L, & Blandford, R. 1976, ApJ, 207, 574

Sosin, C., & King, I.R. 1997, AJ, 113, 1328

Spitzer, L 1987, "Dynamical Evolution of Globular Clusters", Princeton University Press, 191

Stappers, B.W., Bailed, M., Lyne, A.G., Manchester, R.N., D'Amico., N., Tauris, T.M., Lorimer, D.R., Johnston, S., & Sandhu, J.S. 1996, ApJ, 465, L119

Stappers, B.W., van Kerkwijk, M.H., Bell, J.F., & Kulkarni, S. R. 2001, ApJ, 548, L183

Stetson, P.B. 1994, PASP, 106, 250

Stetson, P.B. 2000, PASP, 112, 925

Tauris, T.M., & Savonije. G.J. 1999, A&A, 350, 928

Taylor, J.M., Grindlay, J.E., Edmonds, P.D., & Coll, A.M. 2001, ApJ, 553, L169

Thompson, C., Blandford, R.D., Evans, C.R., & Phinney, E.S. 1994, ApJ, 422, 304

Thorsett, S.E., & Chakrabarty, D. 1999, ApJ, 512, 288

Tomkin, J., Lemke, M., Lambert, D.L., & Sneden, C. 1992, AJ, 104, 1568

Trager, S.C., King, I.R., & Djorgovski, S. 1995, AJ, 109, 1912

Trenti, M., Ardi, E., Minesinghe, S., Hut, P. 2007 MNRAS 374, 857

Unavane, M., Wyse, R.F.G., & Gilmore, G. 1996, MNRAS, 278, 727

van den Heuvel, E.P.J. & Bitzaraki, O. 1995, A&A, 297, L41

van der Klis, M., Clausen, J.V., Jensen, K., Tjemkes, S., & van Paradijs, J. 1985, A&A, 151, 322

Ventura, P., D'Antona, F., Mazzitelli, I., & Gratton, R. 2001, ApJ, 550, 65

Verbunt, F. 1987, ApJ, 312, L23

Verbunt, F. 1993, ARA&A, 31, 93

Verbunt, F. 2006, AIPC, 797, 30

Xie, B., Pryor, C., Gebhardt, K. & Williams, T. 2002, Bulletin of the American Astronomical Society, 201, 706

Wijnands, R., & van der Klis, M. 1998, Nature, 394, 344

Wood, M. A. 1995, LNP Vol. 443: White Dwarfs, 41